Response to Editor

Dear Nathalie,

Many thanks you for your timely response. We are grateful that you will accept our manuscript after some last adjustments.

We explain in more detail why we think that the Bergsee record is not suited for our composite figure (Fig. 4). We had long discussions about that in the author team and at the end, everybody was in favor of staying with our own figure suggestion. To come to this decision we consulted and produced new figures on the Bergsee record we would like to share with you. Below we provide our reasons with further details.

Kind regards,
Fabian Rey & Co-authors

"First remove "see " before the citations in the text, it is not necessary"
We changed this as requested before all citations and also in front of most hints to figures and tables.

"Secondly, I am not convinced by your arguments for your refusal to draw the Bergsee curves in front of your data in Fig.4. I do not understand. It will reinforced your gradient and your interpretation as in the Bergsee pollen data show the same pattern as in the north Switzerland. could you please envisage to test a figure with a synthetic diagram of Begsee on the left of your figure 4. or please tell me if it is impossible for you to do that."
We would prefer to not show the Bergsee record in our composite Fig. 4. This point has led to many discussions in the research team. We re-assessed our reasons and came to the conclusion that they are still valid. The *Juniperus* peak at Bergsee has a clear age offset by more than 500 years, which is either a chronological deficit or a local (anomalous) feature that is not shared in our region (southern Central Europe). We attached Fig. 3 from Duprat-Oualid et al. 2017 to show this problem (Fig. 1 below). They mark the OD-Bölling transition with a black line which is at around 14,100 cal BP in their figure. However, in the results part Duprat-Oualid and colleagues write the following:
"Both pollen diagrams (Figs 3 and 5) underline the transition between the Last Glacial and the Lateglacial at 14.7k cal a BP. Pollen dynamics of the Lateglacial and early Holocene (14.7–11.7k cal a BP) are already well documented for the region (Rösch, 1992; Eusterhues et al., 2002): dwarf shrubs are first established, rapidly replaced by Betula (i.e. Bölling: 14.7–14k cal a BP) and followed by Pinus (Alleröd: 14–12.7k cal a BP). According to the pollen data and the chronology, the period corresponding to GI-1 is clearly manifest in the Bergsee sequence (Fig. 3, BPZ-4)."
Here, they explain the classical transition from *Juniperus* shrublands to boreal forests from 14,700 cal BP onward, which is indeed valid for our study region. However, to come to this conclusion they use the calibrated radiocarbon ages available from the literature that are in fact perfectly correct. Their own data however do not show this timing according to their Fig. 3 (see below Fig. 1), which is very surprising to us. Indeed their *Juniperus* peak is at around 14,000 cal BP instead of the regionally valid 14,600 cal BP (thus ca. 600 years too young). Chronostratigraphically

even more problematic is their *Betula* peak at ca. 13,300 cal BP, which in the region has a correct initial age of ca. 14,400–14,300 cal BP. In the Bergsee record the *Betula* expansion seems thus 1000 years too young, if compared to all other well-dated records from the region. Indeed, the subsequent *Pinus* expansion occurred at ca. 13,800–13,700 cal BP in the region, while in the Bergesee record it is again 800–900 years too young, at ca. 13,000-12,800 cal BP. To illustrate this chronological issue of the Bergsee record, we show the offset of 1000 years in forest expansion (13,400 vs. 14,400 cal. BP) with arrows (Fig. 2, below), if compared to Moossee and other records from our study region such as Soppensee or Gerzensee. Given that the Bergsee record only has one radiocarbon date (black box on the left of Fig. 2 shown below) for the time interval of interest (our Fig. 4), it might well be that the cause for this huge age offset are chronological uncertainties. Interestingly, the median age of the radiocarbon date, which is 14,600 cal BP (Table 1 in Duprat-Oualid et al. 2017), would fit very well with our data and all the regional evidence. However, unfortunately Duprat-Oualid et al. 2017 chose a smooth spline age-depth model (Fig. 2 in Duprat-Oualid et al. 2017) instead of e.g. linear interpolation, a procedure which is known to create uncertainties, if few dates are available (the closest neighboring dates are extremely distant at ca. 11,000 and 20,000 cal BP). Indeed, with these few dates, the age-depth model of Bergsee is forced to run through the very edge of the calibration range of the only available date for this period at ca. 14,200 cal BP, which is a fully correct procedure, but biostratigraphically (on the basis of the available radiocarbon-dated records) unrealistic. On the basis of these reflections and discussion, our author team came again to the conclusion that the Bergsee record is unsuited for our synthesis figure, and we very much hope to have convinced you about this issue, which is very important to us.

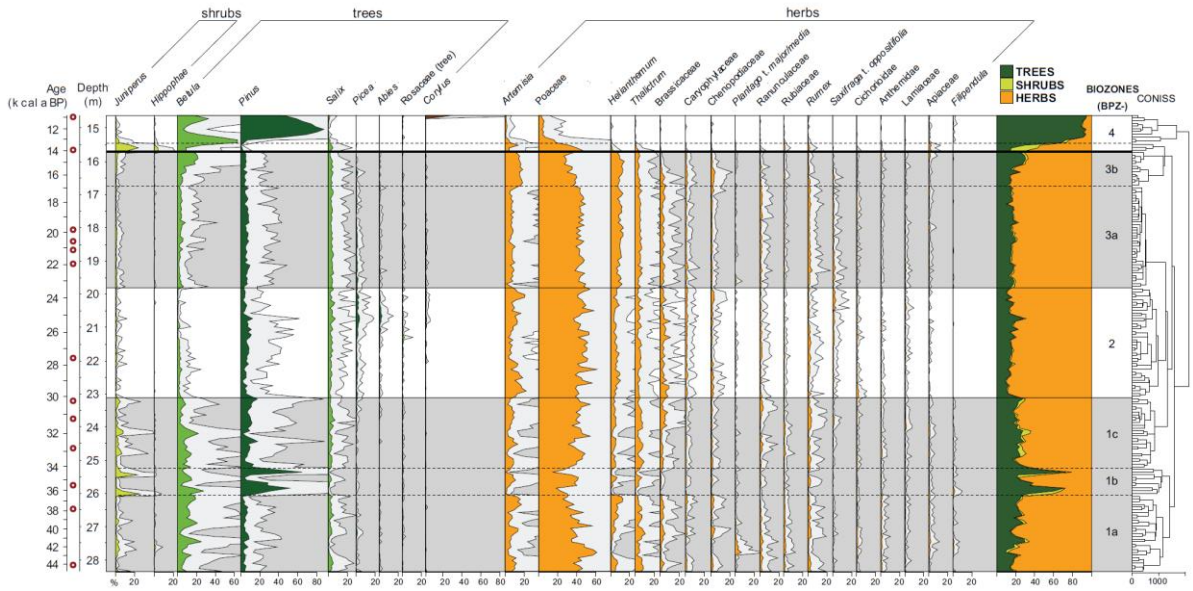

Fig. 1 Bergsee pollen record (Duprat-Oualid et al. 2017). The black line is the OD-Bölling transition. Red circles are the position of the radiocarbon dates.

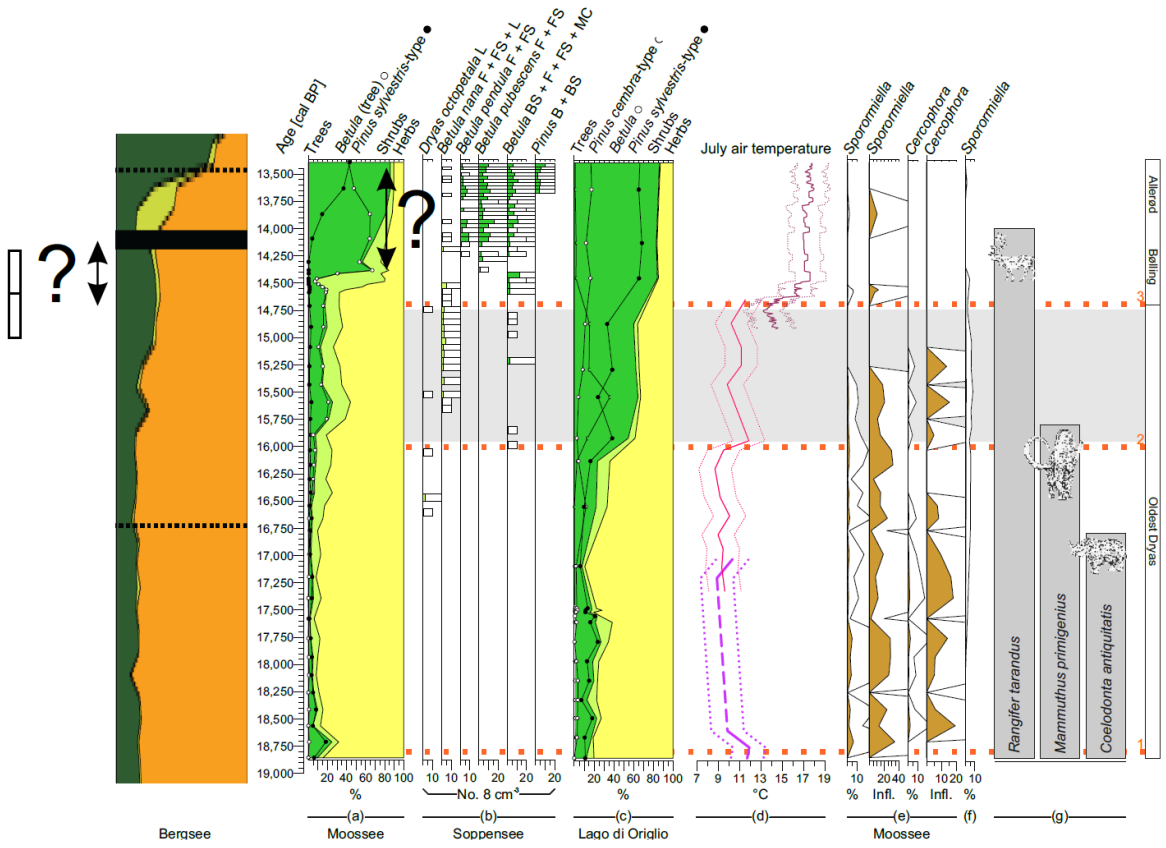

Fig. 2 Comparison of the main pollen diagram from the Bergsee record with our composite figure. Green is tree pollen, light green is shrub pollen and yellow or orange is herbaceous pollen. Arrows mark age offsets. Question marks show dating uncertainties. The black box is the position of the radiocarbon date from Bergsee that has a biostratigraphically correct median of 14,600 cal BP (age at Moossee is ca. 14,600 cal BP too), but was modelled centuries to young.

"Thirdly, I do not refuse the comparison with Sofular cave but I think that there are nearest speleothem records in Europe that may be also good candidate for comparison. Tell me why you use this one to compare to Switzerland record or change the record."

Sofular cave is actually the closest speleothem record covering the entire past 19,000 years. Of course they are records that would be closer (e.g. Bourgeois–Delaunay, France; Katerloch, Austria; Hölloch, Germany; Corchia, Italy) but they are covering either older time intervals (Bourgeois–Delaunay, Corchia) and/ or only time windows that are too short (Katerloch, Hölloch, Corchia) to understand and explain the long-term trends we want to show in Fig. 5. Furthermore, the record from Sofular cave fits very well into our North-South gradient discussion since it also shows a clear trend after 16,000 cal BP (beside onset of the Bölling, YD and onset of the Holocene), which is novel.

Climate impacts on vegetation and fire dynamics since the last deglaciation at Moossee (Switzerland)

Fabian Rey[1,2,3], Erika Gobet[1,2], Christoph Schwörer[1,2], Albert Hafner[2,4], Sönke Szidat[2,5], Willy Tinner[1,2]

[1]Institute of Plant Sciences, University of Bern, CH-3013 Bern, Switzerland
[2]Oeschger Centre for Climate Change Research, University of Bern, CH-3013 Bern, Switzerland
[3]Geoecology, Department of Environmental Sciences, University of Basel, CH-4056 Basel, Switzerland
[4]Institute of Archaeological Sciences, University of Bern, CH-3012 Bern, Switzerland
[5]Department of Chemistry and Biochemistry, University of Bern, CH-3012 Bern, Switzerland

Correspondence to: Fabian Rey (fabian.rey@unibas.ch)

Abstract. Since the Last Glacial Maximum (LGM, end ca. 19,000 cal BP) Central European plant communities were shaped by changing climatic and anthropogenic disturbances. Understanding long-term ecosystem reorganizations in response to past environmental changes is crucial to draw conclusions about the impact of future climate change. So far, it has been difficult to address the post-deglaciation timing and ecosystem dynamics due to a lack of well-dated and continuous sediment sequences covering the entire period after the LGM. Here, we present a new palaeoecological study with exceptional chronological time control using pollen, spores and microscopic charcoal from Moossee (Swiss Plateau, 521 m a.s.l.) to reconstruct the vegetation and fire history over the last ca. 19,000 years. After lake formation in response to deglaciation, five major pollen-inferred ecosystem rearrangements occurred at ca. 18,800 cal BP (establishment of steppe tundra), 16,000 cal BP (spread of shrub tundra), 14,600 cal BP (expansion of boreal forests), 11,600 cal BP (establishment of first temperate deciduous tree stands composed of e.g. *Quercus, Ulmus, Alnus*) and 8200 cal BP (first occurence of mesophilous *Fagus sylvatica* trees). These vegetation shifts were released by climate changes at 19,000, 16,000, 14,700, 11,700 and 8200 cal BP. Vegetation responses occurred with no apparent time lag to climate change, if the mutual chronological uncertainties are considered. This finding is in agreement with further evidence from Southern and Central Europe and might be explained with proximity to the refugia of boreal and temperate trees (< 400 km) and rapid species spreads. Our palynological record sets the beginning of millennial-scale land use with periodically increased fire and agricultural activities of the Neolithic period at ca. 7000 cal BP. Subsequently, humans rather than climate triggered changes in vegetation composition and structure. We conclude that *Fagus sylvatica* forests were resilient to long-term anthropogenic and climatic impacts of the mid and the late Holocene. However, future climate warming and in particular declining moisture availability may cause unprecedented reorganizations of Central European beech-dominated forest ecosystems.

1 Introduction

In the near term, rapid climatic and environmental changes hold a substantial risk to modify irreversibly plant ecosystems in Europe (Schumacher and Bugmann, 2006; Kovats et al., 2014; Bugmann et al., 2015). Quantifying the response or resilience of ecosystems to environmental change in the past largely improves our capacity to assess future impacts of climate and global change (Henne et al., 2015). Specifically, palaeoecological data offer the great opportunity to study long-term climate-vegetation interactions under conditions that exceed the variability and duration recorded in historical archives or through measurements and experiments (Willis and Birks, 2006; Birks et al., 2016; Henne et al., 2018).

During the Last Glacial Maximum (LGM), large areas in Central and Southern Europe around the Alps, in the Jura Mountains, the Black Forest, the Vosges and the Apennines were covered by ice (Ehlers and Gibbard, 2004; Bini et al., 2009; Ehlers et al., 2011; Seguinot et al., 2018). The subsequent deglaciation is generally well-studied, however, timing issues remain due to dating uncertainties (e.g. Wirsig et al., 2016). Recent advances in Accelerator Mass Spectrometry (AMS) radiocarbon dating offer the possibility to produce reliable results with relatively small chronological uncertainties, when using samples with extremely low carbon contents (Szidat et al., 2014; Uglietti et al., 2016). Radiocarbon dates on terrestrial plant remains extracted from the very bottom of lake sediments from sites close to the LGM glacier margins may thus help to refine the onset of deglaciation. However, only very few sedimentary records providing reliable deglaciation ages (i.e. no bulk dating, only terrestrial macrofossils, ~~see~~ Finsinger et al., 2019) are available so far from the peri-alpine belt (e.g. Lister, 1988; Laroque and Finsinger, 2008; Lauterbach et al., 2012). Similarly, well-dated pollen profiles from Western and Central Europe covering the first two millennia of the Oldest Dryas (ca. 19,000–17,000 cal BP) are almost absent and the existing chronologies are therefore often inadequate (e.g. Woillard, 1978; Welten, 1982; Ammann and Tobolski, 1983; de Beaulieu and Reille, 1984; de Beaulieu and Reille, 1992). Conversely, the temporal evolution of the vegetation after 17,000 cal BP is better known (e.g. Lotter, 1999; Tinner et al., 1999; Duprat-Oualid et al., 2017; Rey et al., 2017). Various sites south of the Alps indicate a first afforestation after 16,000 cal BP (e.g. Vescovi et al., 2007) and the main cause has been identified as the post-Heinrich event (HE) 1 warming (Samartin et al., 2012). At around 16,000 cal BP shrub and probably even tree birches expanded into the steppe tundra north of the Alps (Lotter, 1999; Duprat-Oualid et al., 2017; Rey et al., 2017), forming open parklands or shrub tundra. North of the Alps, forests expanded after 14,700 cal BP as a consequence of the Bølling warming (~~see~~ Ammann et al., 2013; van Raden et al., 2013), a process which was delayed by almost 1500 years compared to the lowlands south of the Alps (Vescovi et al., 2007). The reasons causing this long time-lag are not yet fully understood but might be related to a strong latitudinal temperature gradient and the presence of large ice masses (Heiri et al., 2014). The subsequent forested Late Glacial and Holocene vegetation history of the Swiss Plateau is best-studied and the chronological framework is rather robust (e.g. Lotter et al., 1999; Wehrli et al., 2007; Rey et al., 2017).

Taken together, despite the long tradition of palaeoecological research in Central Europe with quite a high density of well-dated and highly resolved studies, a profound modern assessment of the major vegetation changes and their main causes is currently lacking for the complete post-LGM time period. Here, the novel Moossee record has the great potential to shed new light on the timing of lake formation and on important vegetation reorganizations for the past 19,000 years in a central area of the Swiss Plateau. In this study we aim (1) to reconstruct the timing of deglaciation and the establishment of first pioneer vegetation around the lake after the LGM, (2) to identify major postglacial changes in ecosystem evolution on the Swiss Plateau and to assess their causes, (3) to discuss the resilience and the vulnerability of Central European lowland forests in the past to inform the near future and (4) to emphasize the utility of exceptional temporal precision and resolution.

2 Study site

Moossee is a small eutrophic lake at 512 m a.s.l. (47°1′17.0′’N, 7°29′1.7′’E) located on the Swiss Plateau within the periphery of the Swiss capital Bern. The study area geologically belongs to the carbonate-rich molasse region with predominantly sandstone in between the Jura Mountains in the north and the Alps in the south (Schmid et al., 2004). The lake formed after the retreat of the Rhône glacier after the LGM and has a surface area of 0.31 km^2,

with one main inflow in the west and one outflow in the east (Fig. 1b). The maximum water depth is 22 m, with generally anoxic waters in the hypolimnion below 12 m (Guthruf et al., 1999). The lake used to be at least ten times larger in the past, but its size has shrunk due to peat formation over the millennia and artificial lake level lowering (by 4–5 m) since the late 18th century. Lake levels were lowered to drain the wetlands for peat exploitation and to gain agricultural land (von Büren, 1943; Guthruf et al., 1999; Harb, 2017, Fig. 1b). The climate at Moossee is oceanic with mean annual temperatures of 8.8 °C and an annual rainfall of 1059 mm (data from from Bern-Zollikofen at ca. 3 km distance, MeteoSwiss, 2017). July is the warmest month with a mean temperature of 18.6 °C. The wettest months are May–August with more than 100 mm of rainfall per month (MeteoSwiss, 2017).

Alnus glutinosa and *Fraxinus excelsior* form fragmented stands along the lake shore, whereas mixed *Fagus sylvatica* forests are dominant on the more elevated surrounding hills. The remaining and rather flat areas are either intensively used for agriculture or covered by settlements and infrastructure. The earliest archaeological findings around the lake date back to the Magdalenien and the Upper Palaeolithic ca. 15,950–14,750 cal BP (14,000–12,800 cal BC). At that time, two reindeer hunter camps (Moosbühl I and II) were located at the former lake shore (Bullinger et al., 1997; Harb, 2017; Nielsen, 2018, Fig. 1b). Many finds, including preserved lake-shore villages, are known from the Neolithic from ca. 6450 cal BP on (4500 cal BC), impressively documenting the strong prehistoric human activities in the region (Hafner et al., 2012; Harb, 2017, Fig. 1b). The following Bronze Age and Early Iron Age is represented with scattered artifacts and grave mounds in the proximity of the lake (Harb, 2017). In the Bern area the first urban centre was the oppidum Brenodor, which was built during the Late Iron Age or La Tène period (Ebnöther and Wyss, 2004). It persisted during the Roman Age as vicus Brenodurum. The Iron Age and Roman ruins (e.g. fortifications, bath, amphitheatre) are still visible in the town on the Enge peninsula at 5 km distance from Moossee (Ebnöther and Wyss, 2004). Finally, the medieval city centre, which is part of the UNESCO World Heritage "Old City of Bern", was founded in 1191 AD around the Nydegg castle that already existed before (Hofer and Meyer, 1991).

3 Materials and methods

3.1 Coring and chronology

Six parallel sediment cores were retrieved at 19 m water depth with a UWITEC piston corer in the eastern part of the lake. Three cores (Moos A–C, core diameter: 60 mm, core length: 300 cm) reached coring depths of ca. 17.5 m. For the other three cores (Moos F–H, core diameter: 90 mm, core length: 200 cm), due to higher friction it was only possible to recover the uppermost 7 m. A master sequence with a total length of 16.44 m was defined using the Moos F–H cores for the uppermost 7 m and the Moos A–C cores for the remaining part. The sediment material below 13.5 m was not analyzed due to frequent sand layers in the lowermost part resulting in very low pollen concentrations.

The chronology is based on 62 radiocarbon dates on terrestrial plant macrofossils and the Laacher See Tephra (LST; ~~see~~ Table 1). The radiocarbon content of terrestrial plant remains was measured at the LARA laboratory at the University of Bern using accelerator mass spectrometry (AMS, ~~see~~ Szidat et al., 2014). None of the 62 radiocarbon dates was rejected. From 435–691 cm, additional varve counts were applied to refine the chronology. Here, the program OxCal 4.3 (V-sequence, Bronk Ramsey, 1994, 1995, 2001; Bronk Ramsey et al., 2001) and the IntCal13 calibration curve (Reimer et al., 2013) were used to estimate the age-depth model and its 95 % (2σ) probabilities (partly published, ~~see~~ Rey et al., 2019b). For the remaining part (0–435 cm and 691–1335 cm), a

smooth-spline curve (smoothing level = 0.3) was calculated with the program clam 2.2 (Blaauw, 2010) to assess the final age-depth model (Fig. 2). The modelled curve runs within the 95 % (2σ) probabilities of the calibrated radiocarbon ages and the 2σ confidence envelope of a generalized mixed-effect regression that includes both, sample depth and age uncertainties (GAM, Heegaard et al., 2005).

3.2 Pollen, non-pollen palynomorphs and charcoal analysis

A total of 514 samples for pollen and microscopic charcoal analyses were taken from the sediment core from 1296 cm to the top. The standard sampling was 1 cm^3 every 10 cm. A higher resolution was implemented for the Oldest Dryas (18,800–14,700 cal BP), for the Early Bølling (14,700–14,400) and for the Neolithic–Mid Bronze Age (7400–3200 cal BP, ~~see~~ Rey et al., 2019a). All palynological samples were treated with HCl, KOH, HF, acetolysis, sieved with a mesh size of 0.5 mm and mounted in glycerine following standard approaches (Moore et al., 1991). *Lycopodium* tablets (University of Lund batch no. 1031 with 20,848 ± 3457 spores per tablet) were added before the chemical treatment to estimate microfossil concentrations (Stockmarr, 1971). Pollen, spores and non-pollen palynomorphs (NPPs) were identified under a light microscope at 400× magnification using palynological keys (Moore et al., 1991; Beug, 2004), photo atlases (Reille, 1992) and the reference collection at the Institute of Plant Sciences (University of Bern). *Betula nana* and tree *Betula* pollen grains were separated following Birks (1968) and Clegg et al. (2005). Cerealia-type pollen was identified according to size, pore diameter and annulus thickness (~~see~~ Beug, 2004).

Pollen and spores were used to infer extra-local to regional vegetation dynamics (Conedera et al., 2006). A minimum pollen sum of 500 terrestrial pollen grains per sample was counted. For the lowest part of the sediment core, the minimum pollen sum was > 100 terrestrial pollen grains due to the low pollen concentration in the bottom part of the sediment sequence. A total number of 165 terrestrial pollen types were identified. *Sporormiella* and *Cercophora* (coprophilous fungal spores, ~~see~~ e.g. van Geel et al., 2003) was used as a proxy for grazing activities of herbivores (e.g. Gill et al., 2013; Rey et al., 2017) and livestock farming (e.g. Rey et al., 2013; Schwörer et al., 2015). The pollen and NPP results are presented in percentages of the terrestrial pollen sum excluding *Cannabis sativa* pollen (due to artificial pollen input by hemp retting, ~~see~~ Ranalli and Venturi, 2004) and pollen of aquatic plants (Fig. 3). For *Sporormiella* and *Cercophora*, influx values (spores cm^{-2} yr^{-1}) are also shown (Fig. 4).

We used microscopic charcoal as a proxy for regional fire activity (Tinner et al., 1998; Adolf et al., 2018). Particles > 10 µm and < 500 µm were analyzed and counted on the pollen slides following Tinner and Hu (2003) and Finsinger and Tinner (2005). The data are presented as microscopic charcoal influx values (particles cm^{-2} yr^{-1}, Fig. 3). Local pollen assemblage zones (LPAZ) were identified using optimal sum-of-squares partitioning (Birks and Gordon, 1985), while statistically significant zones were determined following the broken-stick method (Bennett, 1996). For simplification and comparison with the LPAZ, we added important climatic breaks (1–5) that are either related to temperature changes (breaks 1–4, see compilation of chironomid-based July air temperature estimate since the LGM in Finsinger et al. (2019) or increases of moisture availability e.g. Tinner and Lotter, 2001; Joannin et al., 2013). The evidence for the temperature and moisture breaks comes from previous studies: break 1 corresponds to the onset of the Oldest Dryas (19,000 cal BP, e.g. Wirsig et al., 2016); break 2 to the post-HE-1 warming (16,000 cal BP, e.g. Samartin et al., 2012); break 3 to the onset of the Bølling (14,700 cal BP, e.g. van Raden et al., 2013); break 4 to onset of the Holocene (11,700 cal BP, e.g. Heiri et al., 2015); and break 5 to the 8.2 ka event (8200 cal BP, e.g. Tinner and Lotter, 2001; Joannin et al., 2013). This climate synopsis allows for the first time a tentative regional assessment and discussion of climate amplitude variation and its impacts on

vegetation for the past 19,000 years. All calculations were run with the program R statistics (R Development Core Team, 2018). The data were plotted with the use of the programs Tilia 2.0.60 and CorelDraw.

3.3 Biodiversity estimations and ordination analysis

We first applied rarefaction analysis to calculate palynological richness (PRI), which is frequently used as a proxy for local to regional species richness (e.g. Birks and Line, 1992; Odgaard, 1999; Schwörer et al., 2015; Birks et al., 2016; Rey et al., 2019a). Rarefaction analysis assesses the number of taxa per sample after setting a constant minimum terrestrial pollen sum (Birks and Line, 1992), which was 116 in our case. Subsequently, the probability of interspecific encounter (PIE, Hurlbert, 1971) was taken as a measure of palynological evenness (van der Knaap, 2009). To assess distortion biases related to pollen production and dispersal on PRI (e.g. through high-pollen producers such as *Pinus sylvestris*, *Corylus avellana*), evenness-detrended palynological richness (DE-PRI) was calculated (~~see~~ Colombaroli and Tinner, 2013). The aim of this procedure is to remove the evenness trend from PRI by applying an ordinary least square regression (OLS) between PRI and PIE and adding the deriving residuals (PRI - PIE) to the original PRI values (residuals + PRI). Only if PRI and DE-PRI indicate comparable trends and changes, we suppose that PRI is uninfluenced by evenness effects and thus primarily reflects species richness. The program R statistics (R Development Core Team, 2018) was applied for the calculations.

We used ordination analysis (Birks and Gordon, 1985; Ter Braak and Prentice, 1988) to identify gradients in vegetation composition over time using the program Canoco 5 (Šmilauer and Lepš, 2014). We first performed a detrended correspondence analysis (DCA, Birks and Gordon, 1985) by segments without down-weighting of rare species to assess the appropriate response model (i.e. unimodal vs. linear) for our pollen percentage data. Since there is important turnover in the species composition as indicated by the rather long gradient length of the first DCA axis (3.41 SD), we retained the unimodal response model (DCA, Šmilauer and Lepš, 2014).

4 Results and interpretation

4.1 Lithology and sedimentation

The lowermost part of the sediment sequence (1644–1300 cm, 19,000 cal BP and older), which was not analyzed for pollen and microscopic charcoal, consists of clay and sand layers. From 1300 cm (19,000 cal BP) upward, the sediment content changes to silty clay without sand layers until 980.5 cm (14,400 cal BP). According to the age-depth model (Fig. 2), the sedimentation rate is steadily decreasing at the same time, suggesting the establishment of relatively stable soil conditions shortly after deglaciation. From 980.5 cm (14,400 cal BP) to the top, the sediment consists of calcite-rich fine detritus gyttja. Between 712–429 cm (7550–2650 cal BP, ~~see~~ Rey et al., 2019a, b) the sediment is continuously varved. Some additional partly laminated sections are present at 980.5–768 cm (14,400–8900 cal BP) and at 415−134 cm (2350–300 cal BP). The sedimentation rate becomes rather stable from 980.5 cm (14,400 cal BP) onward and stays more or less constant until 429 cm (2650 cal BP). This stabilization is probably linked to forests growing in the catchment reducing the total erosional input. The uppermost 429 cm (2650 cal BP to the present) are characterized by a steep increase of the sedimentation rate, which is most likely related to increased erosion in response to forest openings and agricultural activities in the catchment of the lake.

4.2 Vegetation and fire history

The pollen sequence (Fig. 3) is subdivided into 21 local pollen assemblage zones (LPAZ) and five subzones (Moos-1a, 1b, 20a, 20b and 20c). The high number of statistically significant zones, especially in the upper part of the diagram (i.e. at 7300–2900 cal BP) is related to the exceptionally high sample resolution and the rather strong vegetation changes.

Herbaceous pollen grains from Poaceae, *Artemisia*, *Helianthemum*, *Thalictrum*, Chenopodiaceae, Rubiaceae and *Saxifraga aizoides*-type are dominant at the end of the LGM (climatic break 1, ca. 19,000–18,800 cal BP, LPAZ Moos 1a, Wirsig et al. 2016; Finsinger et al. 2019). This indicates the establishment of open steppe/ tundra vegetation in the region including some first pioneer dwarf shrubs such as *Salix herbacea* (macrofossils found, ~~see~~ Table 1), quickly after deglaciation. The increased pollen percentages of *Pinus sylvestris*-type (up to 18 %) may be interpreted as long-distance transport from forested, formerly unglaciated areas and single grains of *Abies alba* and *Picea abies* might point to reworking processes probably due to persisting meltwater influence of the retreating Rhône glacier. High values of *Sporormiella* (percentages up to 6 %, influx up to 35 spores cm^{-2} yr^{-1}, ~~see~~ Fig. 4) as a proxy for local grazing (van Geel, 2006) may be indicative of the presence of Pleistocene megafauna such as *Mammuthus primigenius* (wolly mammoth), *Coelodonta antiquitatis* (wolly rhinoceros), *Rangifer tarandus* (reindeer) and others that were preferentially living in the cold steppe environment at that time (e.g. Nielsen, 2013). Charcoal influx values are extremely low (< 50 particles cm^{-2} yr^{-1}), suggesting rare or almost no fire activity in the region due to scarce vegetation cover.

From 18,800–16,000 cal BP (between climatic breaks 1 and 2, LPAZ Moos-1a), the pollen record indicates that an open, species-rich (see *Gypsophila repens*-type and *Rumex acetosa*-type pollen curves), herb dominated steppe tundra persisted around Moossee. A first slight increase of shrub pollen percentages (from 7 to 14 %) mainly from *Betula nana*, *Salix*, *Juniperus* and *Ephedra fragilis*-type suggest that patches of dwarf shrubs established in the region after 17,000 cal BP. This is underlined by findings of *Betula nana* remains (~~see~~ Table 1). *Sporormiella* values remain high (at 1–5 % respectively around 20 spores cm^{-2} yr^{-1}) and *Cercophora* values peak (at 2.5 % respectively 20 spores cm^{-2} yr^{-1}, ~~see~~ Fig. 4), pointing to prevalence of wild animals grazing at the lake. Charcoal influx values stay low (10–40 particles cm^{-2} yr^{-1}), suggesting that regional fires were still absent.

Pollen percentages of tree *Betula* are markedly increasing (values up to 21 %) after the end of HE-1 (climatic break 2) during LPAZ Moos-1b (16,000–14,600 cal BP), suggesting the regional establishment of tree *Betula* stands or woods. Shrub pollen percentages (i.e. *Betula nana*, *Ephedra fragilis*-type, *Salix*, *Juniperus* and *Hippophaë rhamnoides*) stay at 12–20 %, whereas non-arboreal pollen (= NAP) values decrease but remain very high (55–75 %, see pollen percentages of *Artemisia*, *Heliathemum*, *Thalictrum* and Chenopodiaceae). This change points to an expansion of shrub tundra with *Betula nana*, *Salix*, *Juniperus* and maybe even some small growing *Betula* trees into the catchment of Moossee and is possibly related to climate warming after 16,200 cal BP (Samartin et al., 2012; Finsinger et al., 2019). The values of *Sporormiella* and *Cercophora* diminish and fade out at the same time, suggesting that some of the megaherbivores producing a lot of dung (e.g. *Mammuthus primigenius*) may have become extinct locally (~~see~~ Nielsen, 2013; Cupillard et al., 2015). Charcoal influx prevail at low values (< 40 particles cm^{-2} yr^{-1}), indicating that despite higher total biomass and fuel availability, regional fire activity did not increase.

Pollen data suggest that at the onset of the Bølling warming at ca. 14,700 cal BP (climatic break 3; van Raden et al., 2013; Finsinger et al., 2019), juniper shrub thickets or woods expanded (*Juniperus* pollen percentages > 65 %) and other woody taxa (peaks of *Hippophaë rhamnoides* and *Salix* pollen), leading to the gradual replacement of

shrub and steppe tundra by boreal birch-pine forests (LPAZ Moos-2, ca. 14,600–14,400 cal BP, Fig. 3). Mixed *Juniperus* shrublands persisted for the subsequent 150–200 years until the onset of a marked expansion of tree *Betula* (pollen > 60 %), suggesting the establishment of birch forests around Moossee (ca. 14,400–13,750 cal BP, LPAZ Moos-3). This birch forest expansion resulted in an essential change in lithology (see Sect. 4.1). Subsequently, pollen of *Pinus sylvestris*-type steadily increases, suggesting the establishment of birch-pine forest around the lake (LPAZ Moos-4, 13,750–11,050 cal BP). These boreal forests prevailed through the Allerød warm period (13,900–12,900 cal BP, van Raden et al., 2013), the subsequent Younger Dryas (12,700–11,700 cal BP, Finsinger et al., 2019) and during the first centuries of the Holocene, as suggested by the pollen assemblages. However, the dominance of *Pinus sylvestris*-type and the decrease of *Betula* pollen after 12,900 cal BP, followed by an increase of herb pollen (≤ 20 %, see Poaceae, *Artemisia*) and *Juniperus* pollen (2–3 %), points to a transformation of closed mixed boreal forests into more open, pine-dominated parklands. We interpret this change as a consequence of climate cooling during the Younger Dryas. *Sporormiella* fungal spores are only occurring sporadically which might indicate a low grazing activity in the close vicinity of the lake. Charcoal influx values increase temporarily (> 1000 particles cm^{-2} yr^{-1}) at the onset of mixed birch-pine forest formation and remain at elevated but stable values (> 100 particles cm^{-2} yr^{-1}), suggesting slightly enhanced fire activity after 13,400 cal BP. The re-establishment of closed mixed birch-pine forests occurred shortly after the onset of the Holocene (climate break 4, ca. 11,700 cal BP, Heiri et al., 2015; Finsinger et al., 2019) as indicated by the increase of arboreal pollen (> 80 %). Continuous curves of *Quercus*, *Alnus glutinosa*-type, *Corylus avellana* and *Ulmus* pollen suggest the presence of first temperate forest stands likely in response to the Holocene climate warming already at ca. 11,700–11,500 cal BP. However, temperate trees and shrubs (i.e. *Quercus*, *Corylus avellana*, *Ulmus*, *Tilia*, *Acer* and *Hedera helix*) expanded only after ca. 11,100 cal BP (LPAZ Moos-5, 11,050–8600 cal BP) as indicated by the pollen percentages, replacing the boreal forests within ca. 200–400 years (decrease of tree *Betula* and *Pinus sylvestris*-type pollen). This continental open forest and shrub vegetation was advantaged by the continental climate with hot and dry summers of the Early Holocene (Tinner and Lotter, 2001; Heiri et al., 2015). However, at 9000–8600 cal BP, *Fraxinus excelsior* pollen percentages increase and tree pollen indicative of mixed oak forests (*Quercus*, *Ulmus*, *Tilia*, *Acer* and *Fraxinus excelsior*, e.g. Welten, 1982) reach their highest values. Charcoal influx values remain low (Fig. 3), suggesting no significant increase of fire activity during the Early Holocene.

During LPAZ Moos-6 (8600–7250 cal BP), *Corylus avellana* declined, and less heliophilous trees such as *Fraxinus excelsior* and *Tilia* expanded. Likely in response to climate change around 8200 cal BP (climatic break 5, onset of mid Holocene), *Abies alba* and *Fagus sylvatica* pollen reach their empirical limit (i.e. continuous curves at 8400 and 8200 cal BP respectively), suggesting the local establishment of first stands of these tree species (Birks and Tinner, 2016). At the same time, *Alnus glutinosa*-type pollen percentages are steadily increasing, whereas percentages values of mixed oak forest and *Corylus avellana* start to decline. The pollen assemblages suggest that the decline of heliophilous deciduous forests continued after 7250 cal BP (LPAZ Moos-7 to 8, 7250–6400 cal BP), when mixed beech–silver fir forests expanded massively. The general prevalence of mesophilous tree species throughout LPAZ Moos-7 to LPAZ Moos-21 was likely caused by a gradual shift towards more oceanic climate conditions during the Mid–Late Holocene (Tinner and Lotter 2001, 2006), as e.g. reconstructed on the basis of higher lake levels (Magny, 2013; Joannin et al., 2013). However, this long-term dominance of dark mesophilous mixed beech–silver fir forests and the replacement of the formerly widespread mixed oak–linden–elm–maple

forests was also affected by agricultural activities, starting as early as 7000 cal BP (first pollen grains of cultural indicators such as Cerealia-type and *Plantago lanceolata*).

The pollen stratigraphy indicates a stepwise intensification of land use over the millennia with NAP (including cultural indicator pollen) peaking at 5600 cal BP (LPAZ Moos-10, Neolithic), 3850 cal BP (LPAZ Moos-16, Early Bronze Age), 3500 cal BP (LPAZ Moos-18, Middle Bronze Age), 2600 cal BP (LPAZ Moos 20b, Iron Age), 1800 cal BP (LPAZ Moos 20b, Roman Period), 700 cal BP (LPAZ Moos 21, Middle Ages) as well as 200 cal BP (LPAZ Moos 21, Modern times). Each of these land-use phases were generally accompanied by a decrease of tree pollen percentages of late successional *Fagus sylvatica* and *Abies alba* and by the expansion of light-demanding pioneers such as *Betula* trees and *Corylus avellana* shrubs. Mixed beech forests were able to recover after disturbances as suggested by the cyclical shape of the *Fagus sylvatica* curve. However, less resilient trees such as *Tilia, Ulmus, Taxus baccata* and the liana *Hedera helix* could not cope with the repeated forest disruptions mainly through logging, browsing, pollarding and massively increased fire disturbance (~~see~~ Rey et al., 2019a for more details) and were strongly reduced or even disappeared after 4500 to 3500 cal BP.

Most striking are the massive forest openings during the Iron Age/ Roman Period (> 30 % NAP, LPAZ Moos 20b, 2600–1600 cal BP) and from the Middle Ages onward (> 60 % NAP, LPAZ Moos 21, 1050 cal BP – today) which we interpret as the influence of large settlements or urban centres within close proximity (< 8 km) of the lake. The related strong increases of *Quercus* pollen percentages might point to forest management favouring oak for construction and forest pasture (acorn feeding, e.g. Gobet et al., 2000; Wick, 2015). Sporadic *Sporormiella* fungal spores suggest pastoral farming close to the lake. Charcoal influx values generally follow the land-use phases showing two major peaks at 5600 cal BP and 700 cal BP, pointing to two phases of highest fire activity during the past 19,000 years (with up to 26,000 particles cm^{-2} yr^{-1}). The close link to pollen of crops and weeds as well as the related declines of forests, suggest that anthropogenic burning was related to slash-and-burn activities or maintenance of open fields (Tinner et al., 2005).

4.3 Biodiversity reconstruction and ordination

PRI (palnyological richness) and DE-PRI (eveness-detrended palynological richness) are very similar suggesting that overall, PRI is likely unaffected by evenness effects (Fig. 3). The agreement is particularly good during the periods 18,900–14,500 cal BP and 8600 cal BP to present. Here, both PRI and DE-PRI are slightly fluctuating around 15 pollen types per sample. Palynological evenness as inferred from PIE is stable (PIE at 0.8−0.9) in phases where PRI and DE-PRI are in agreement. Significantly lower values (PIE down to 0.5) are recorded from 14,500–8600 cal BP when pollen grains from few taxa are dominant (either *Juniperus*, *Betula*, *Pinus sylvestris*-type or *Corylus avellana*). There, palynological richness drops (PRI < 10 pollen types per sample) whereas DE-PRI stays stable at around 15 pollen types per sample. We thus assume that evenness distortions lead to underestimations of species richness during the period of strong *Juniperus, Betula, Pinus* (ca. 14,500–11,100 cal BP) and *Corylus* dominance (10,800–9000 cal BP, Fig. 3) and that such evenness distortions can be corrected by considering DE-PRI.

Both richness values (PRI, DE-PRI) generally increase (up to 20–25 pollen types per sample) during phases with higher human impact around 5650 cal BP, at 4650 cal BP, around 3850 cal BP and 3500 cal BP as well as after 2600 cal BP. These increases are directly linked to human induced forest openings and the introduction of cultivated plants (e.g. Cerealia-type) as well as the expansion of weeds (e.g. *Plantago lanceolata*), apophytes (e.g. *Urtica*) and heliophilous shrubs (e.g. *Corylus avellana*). Interestingly, also the tundra phase (18,900–14,600 cal

BP) was rather species rich suggesting that PRI and DE-PRI are correlated with openness. A rather low share (25.6 %) of the total pollen data variance is explained by DCA axis 1. Nevertheless, the DCA scores might indicate a signal of openness as the DCA axis 1 goes almost in line with the non-arboreal pollen (NAP) and Poaceae percentages as well as DE-PRI (Fig. 3).

5 Discussion

5.1 Vegetation and fire dynamics from the last deglaciation to the Mid Holocene

The extent of the ice sheet around the Alpine arch during the LGM has been thoroughly studied in the past and the results are available as high-quality maps (e.g. Ehlers and Gibbard, 2004, ~~see~~ Fig. 1a). Radiocarbon dates on terrestrial plant remains preserved in the bottom part of lake sediment sequences can be used to track the onset of deglaciation (Wirsig et al., 2016; Rey et al., 2017). At Moossee, the earliest date gives a calibrated age of 19,200 cal BP (Table 1), which is well in line with the results from other locations around the Alps (Table 2). The unpublished basal dates of Lago di Monate (lab. code BE-8023.1.1) and Gola di Lago (lab. code BE-12286.1.1) derive from new lake sediment cores that are currently under investigation. Interestingly, most of the sites (including Moossee) with calibrated ages older than 18,000 cal years were located rather close to the margin of the former ice sheet (Fig. 1a, Table 2) and below < 500 m of ice (Bini et al., 2009). In contrast, sites with younger radiocarbon ages (17,270–17,820 cal BP, e.g. Lotter and Zbinden, 1989; Tinner et al., 1999; Ravazzi et al., 2014) were either situated below a thicker ice sheet (750–1000 m) or higher up (Gola di Lago: ca. 970 m a.s.l.) and generally further away from the glacier tongues. However, the relatively small age difference between all these sites suggests that the collapse of the ice sheet in the peri-alpine belt occurred within 1000–1500 years, starting not later than 19,300 cal BP at the end of the LGM (23,000–19,000 cal BP for the Alps, Kaltenrieder et al., 2009; Hughes et al., 2013; Samartin et al., 2016). The huge loss of ice masses and the sudden retreat of glaciers were likely controlled by increasing summer insolation (Berger and Loutre, 1991) as well as constantly rising CO_2 and CH_4 concentrations in the atmosphere (Lourantou et al., 2010).

The pollen assemblage shows that pioneer plants colonized the bare grounds around Moossee shortly after glacial retreat (ca. 19,000 cal BP) to form quickly open, species rich and herb-dominated steppe tundra communities (see biodiversity estimations and DCA in Fig. 3). First, arboreal plants (i.e. dwarf shrubs) could establish contemporaneously as indicated by a *Salix herbacea* leaf and *Betula nana* plant remains (~~see~~ Table 1). Comparable vegetation patterns were found at several other sites north of the Alps (e.g. Welten, 1982; Ammann, 1989; Hadorn, 1992; Duprat-Oualid et al., 2017), although only a few have radiocarbon-dated macrofossils of dwarf shrubs such as at Soppensee (*Dryas octopetala* leaves, Lotter, 1999, ~~see~~ Fig. 4), Wauwilermoos (twiglet of Ericaceae, Beckmann, 2004) and Burgäschisee (unidentified arboreal twiglets, Rey et al., 2017) older than 18,000 cal BP. South of the Alps, and close to the LGM refugia (Eastern Po Plain, Kaltenrieder et al., 2009), *Juniperus* shrublands spread on formerly glaciated areas above 400 m a.s.l. (e.g. Tinner et al., 1999, *Juniperus* stomata around 17,500 cal BP, high pollen values before 18,000 cal BP), possibly as a result of climate warming (+ 2.5–3 °C) around ca. 18,800 cal BP (Samartin et al., 2016; Finsinger et al., 2019). Post-LGM climate warming may have also triggered tree species expansions south of the Alps at altitudes ≤ 350 m a.s.l. (*Larix decidua*, *Pinus* sp. and *Betula*) between 17,500–16,000 cal BP (~~see~~ Finsinger et al., 2006; Monegato et al., 2007).

North of the Alps, a first important vegetation shift after the establishment of the steppe tundra occurred at ca. 16,000 cal BP with the expansion of shrub tundra around Moossee (see pollen of tree *Betula*, *Betula nana*,

Juniperus and *Salix*, macrofossils of *Betula nana*). A similar vegetation shift has been recorded elsewhere in the Central European lowlands (Duprat-Oualid et al., 2017; Rey et al., 2017), pointing to a regional establishment of shrub tundra with probably even some tree birch stands. Plant macrofossil data from Soppensee (Lotter, 1999, ~~see~~ Fig. 4), suggest a coeval establishment of dwarf-birch thickets on the Swiss Plateau, while several records of Welten (1982) point to increasing *Betula* abundances. Indeed, the chironomid-inferred July temperature estimates from Lago di Origlio (Samartin et al., 2012, corrected to the altitude of Moossee 521 m a.s.l. assuming a constant modern temperature rate of 6 °C km^{-1}, Livingstone and Lotter, 1998), indicate a July air temperature warming of 2–2.5 °C reaching temperatures of 10–11.5 °C that are suitable for tree growth (Lang 1994) after 16,000 cal BP, even after considering a latitudinal temperature gradient (~~see~~ Figs. 4 and 5, Samartin et al., 2012; Finsinger et al., 2019). Other factors than summer temperatures such as cold air extrusions from the still existing Scandinavian ice sheet in the north and a stronger latitudinal temperature gradient (Heiri et al. 2014) may have prevented the establishment of dense *Betula* forests north of the Alps (Rey et al., 2013). Indeed, south of the Alps, in more sheltered positions, widespread afforestation with *Pinus cembra* and *Larix decidua* started at around 16,500–16,000 cal BP (e.g. Tinner et al., 1999; Hofstetter et al., 2007; Vescovi et al. 2007; Pini et al., 2016, ~~see~~ Fig. 4). At the same time~~South of the Alps~~, sites above 1000 m a.s.l. became ice-free but remained unforested (Vescovi et al., 2007; Pini, 2002), with treeline positions around 800–1000 m a.s.l. (Vescovi et al., 2007).

High and almost continuous abundances of coprophilous *Sporormiella* and *Cercophora* spores from the onset of the Moossee record until ca. 15,250 cal BP could be indicative of Pleistocene megaherbivores (e.g. *Mammuthus primigenius*, *Coelodonta antiquitatis*, *Rangifer tarandus*). Similar results are recorded at Burgäschisee (Rey et al., 2017, ~~see~~ Fig. 4) and fit well with numerous finds of remains of these animals (e.g. bones, tusks, antlers) in the region (Nielsen, 2013; Cupillard et al., 2015). On-site hunter camps located at the former lake shore of Moossee (Fig. 1b), dated to 16,950–14,750 cal BP (14,000–12,800 cal BC, Harb, 2017; Nielsen, 2018), suggest intense hunting. Hunting combined with climate warming may have caused the regional extinctions of *Mammuthus primigenius*, *Coelodonta antiquitatis* and *Rangifer tarandus* during the Late Glacial (~~see~~ Nielsen, 2013; Cupillard et al., 2015), as also evidenced by decreasing numbers dung spores after 15,500 cal BP (Fig. 4).

Juniper shrublands expanded massively at Moossee after ca. 14,600 cal BP (onset of the Bølling) which is in agreement with the well-dated pollen record at Gerzensee (van Raden et al., 2013). Only ca. 200 years later, *Betula* forests took over and completed the initial afforestation which is widely recorded in pollen assemblages across the Swiss Plateau (e.g. Ammann, 1989; Rey et al., 2017) and unambiguously confirmed by *Betula pubescens* and *B. pendula* macroremains at Soppensee (Lotter, 1999, ~~see~~ Fig. 4). Contemporaneously, sites up to 1800 m a.s.l. in the Alps turned ice-free (Welten, 1982; Ilyashuk, et al., 2009). South of the Alps, dense boreal forests with *Pinus sylvestris* and *Betula* established in the lowlands (Vescovi et al., 2007) and the tree line reached at least 1850 m a.s.l. (Tinner and Vescovi, 2007, Marta et al., 2013). This rapid deglaciation in the Alps and the forest expansion in Southern and Central Europe was caused by a sudden ca. 4 °C warming, as indicated by chironomid and stable isotope records (von Grafenstein et al., 1998, 1999; North Greenland Ice Core Project members, 2004; Heiri and Millet, 2005; Larocque and Finsinger, 2008; Fleitmann et al., 2009, ~~see~~ Fig. 5).

After ca. 13,600 cal BP (during the Allerød) mixed birch–pine forests were spreading at Moossee and all across Southern Central Europe (e.g. Clark et al., 1989; Lotter, 1999). In Northern Italy temperate tree stands established, probably in response to increasing summer temperatures (Vescovi et al., 2007, Lotter et al., 2012). The early spread of temperate trees south of the Alps (e.g. *Quercus*, *Tilia*, *Ulmus*) is evidenced by *Quercus* bud scales at Lago Piccolo di Avigliana (Finsinger et al., 2006) and Lago di Ragogna (Monegato et al., 2007). Summer warming

(Heiri et al., 2015, ~~see~~ Fig. 5) may also have triggered the increase of regional forest fires observed at Moossee and elsewhere north of the Alps (Rey et al., 2017).

Boreal forests prevailed around Moossee during the Younger Dryas cold period (ca. 12,600–11,700 cal BP), when a summer temperature cooling of ca. 2–4 °C north of the Alps (Lotter et al., 2000; Heiri et al., 2015; Finsinger et al., 2019, Fig. 5) initiated a recovery of cold steppe–tundra vegetation (e.g. *Artemisia*, Chenopodiaceae). At the same time, late successional pine trees increasingly outcompeted pioneer birch trees, forming open pine-dominated forests, a finding well supported by the macrofossil evidence (Lotter, 1999). Chironomid-based summer temperature reconstructions (Samartin et al., 2012; Heiri et al., 2014) suggest only a marginal cooling in southern Europe, which nevertheless affected temperate trees stands (Tinner et al., 1999; Finsinger et al., 2006; Vescovi et al., 2007). This different magnitude of climate cooling may be related to the sheltered location of these lakes in the lee of the Alps, preventing direct influences from the polar ice masses and the North Atlantic during the Younger Dryas (Samartin et al., 2012; Heiri et al., 2014).

After 11,700 cal BP at the onset of the Holocene, boreal forests became dense in the peri-alpine lowlands (Tinner et al., 1999; Rey et al., 2017). Chironomid-based July temperature estimates (Heiri et al., 2015; Finsinger et al., 2019), other biotic proxies (Lotter et al., 2000, Birks and Ammann, 2000) as well as oxygen isotope records (von Grafenstein et al., 1998, 1999; 2000; Schwander et al., 2000) suggest a sudden warming of 3–4 °C within only ca. 50 years (Tinner and Kaltenrieder, 2005). In response to this rapid and strong climate warming, stands of temperate trees (e.g. *Quercus, Alnus, Ulmus*) established north of the Alps at 11,600–11,100 (Fig. 3) to gradually replace the former mixed pine-birch forests shortly after 11,100 cal BP. By 10,500 cal BP mixed oak–linden–elm–maple forests prevailed. In the forelands of the southern Alps, first mixed oak–linden–elm stands had established already during the Late Glacial, so that the Early Holocene population expansions of temperate trees (e.g. *Quercus, Ulmus, Tilia*) were far more rapid and accomplished by ca. 11,500–11,300 cal BP (Tinner et al., 1999; Finsinger et al., 2006; Vescovi et al., 2007), i.e. 800–1000 years earlier than north of the Alps. This finding is in agreement with process-based dynamic vegetation simulations, which suggest that after a first establishment of boreal and temperate tree stands, population expansions usually last 500–1000 years before coming to a (high) biomass equilibrium with climate (Lotter and Kienast, 1992; Wick and Möhl, 2006; Henne et al., 2011; Schwörer et al., 2014).

The dominance of mixed oak–linden–elm–maple forests over millennia in Central Europe (~~see~~ e.g. Hadorn, 1992; Lotter, 1999; Litt et al., 2009; Rey et al., 2017) was most likely favoured by continental climate as indicated by maximum summer and minimum winter insolation (Berger and Loutre, 1991), 1.5–2 °C warmer summers than today (e.g. Heiri et al., 2015) and generally drier conditions as reflected by lower lake levels (e.g. Magny et al., 2012, ~~see~~ Fig. 5). This forest type persisted until ca. 8500–8000 cal BP (Figs. 3 and 5), when *Abies alba* and *Fagus sylvatica* tree stands established around Moossee. Both tree species are shade-tolerant and competitive under mesophytic conditions (Tinner and Lotter, 2006; Tinner et al., 2013; Lauber et al., 2014). Similarly, *Alnus* and *Fraxinus excelsior*, both well-adapted to wet soils and moist conditions (Lauber et al., 2014; Rey et al., 2017), expanded as well. The establishment and massive spread of mesophilous mixed beech forests after 7500 cal BP (see high number of *Fagus sylvatica* bud scales in Table 1) is well studied on the Swiss Plateau (e.g. Lotter, 1999; Wehrli et al., 2007) and the causes for this change have been intensely discussed in the past (Tinner and Lotter, 2006). Decreasing summer temperatures (Heiri et al., 2015; Finsinger et al., 2019) and increasing moisture availability (e.g. Magny et al., 2011; Magny et al., 2012; Joannin et al. 2013, ~~see~~ Fig. 5) suggest climate as the main trigger of this drastic change in Central European forest composition.

5.2 Vegetation and land-use history during the Mid and Late Holocene

The onset of land use and agricultural activities around Moossee is documented as early as 7000 cal BP by the first cultural indicator pollen such as Cerealia-type and *Plantago lanceolata* (~~see~~ Figs. 3 and 5). Increases of microscopic charcoal, which fall into a phase with fairly closed mixed beech–oak forests (Figs. 3 and 5), suggest a drastic increase of fire activity at the onset of the farming. After 6500 cal BP intensified agricultural activities caused a first dieback of the mixed beech forests. Our interpretation is in good agreement with coeval on-site archaeological evidence (e.g. log boat made of *Tilia* wood; Hafner et al., 2012; Harb, 2017). Many lowland sites south and north of the Alps indicate a contemporaneous opening of the forests. The strong link with increasing fire activities suggests that farmers used fire to gain arable and pastoral land (i.e. slash-and-burn, e.g. Tinner et al., 1999; Kleinmann et al., 2015; Rey et al., 2017, 2019a). Disruption and land-use phases generated typical successional cycles starting with arboreal pioneers (*Corylus avellana*, tree *Betula* and *Alnus*) rapidly spreading after disturbance. These light-demanding pioneers were regularly replaced by *Fraxinus excelsior* and *Ulmus*, which were in turn replaced by late-successional *Fagus sylvatica* and *Abies alba* (e.g. Kleinmann et al., 2015). Most strikingly, a recent high precision and high-resolution study covering three millennia from the Neolithic to the Bronze Age (ca. 7000–4000 cal BP) was able to numerically demonstrate that land-use phases and the subsequent forest successions were regionally to supra-regionally synchronous (Rey et al., 2019a). The most reasonable explanation for such a striking pattern is climate and its influences on human activities. Indeed, Rey et al. (2019a) found that land-use phases generally coincided with warm and dry periods as indicated by lower lake levels in Western Switzerland and Eastern France (Magny, 2013) as well as higher solar irradiance (Steinhilber et al., 2009). This finding underlines that climate may have governed harvest success and through that prehistoric human population densities, an environmental effect that on the long-term was counteracted by stepwise introductions of technological innovations (e.g. metal tools, new crops; Tinner et al., 2003, Wirtz and Lemmen, 2003).

Our palaeobotanical data indicate a steady intensification of agricultural activities during the Late Holocene (from ca. 3850 cal BP onward), which is primarily evidenced in regions on the Swiss Plateau that are climatically favourable for crop production (i.e. < 550 m a.s.l., Ammann, 1989; Hadorn, 1992; Rey et al., 2017). Many tree species were strongly affected by fire disturbance, browsing and/ or overexploitation and some of them (e.g. *Tilia*, *Taxus baccata*) even collapsed completely (Rey et al., 2017). Contrarily, several taxa such as *Quercus* and *Fagus* were promoted as fruit trees (Gobet et al., 2000; Wick, 2015), while others were introduced (e.g. *Juglans regia*, *Castanea sativa*) for the same reason (Tinner et al., 2003; Conedera et al., 2004). Thanks to the combined effects of open land creation and the introduction of new species, total biodiversity increased (Fig. 3), suggesting that human activities related to farming were crucial for the establishment of a mosaic of diverse communities (e.g. hay meadows, orchards, hedges). As a consequence, during the Late Holocene (i.e. the past 5000 years) humans gradually replaced climate as the driving factor of vegetation structure and composition. Woodlands increasingly impoverished, leading to monospecific *Picea*, *Quercus* or *Fagus* forest communities that are best suited for timber, fuel and fodder production. The strong increase of biodiversity in open habitats (meadows, fields, hedges) thus contrasted diversity losses in forests and woodlands (Colombaroli and Tinner, 2013). We can show that in regard to the dominant species, beech forests were able to recover even after the most intense anthropogenic disturbances (e.g. Iron Age, Roman Period, Middle Ages). Therefore, Central European beech may presumably prevail in the future if the amplitude of the anticipated climate warming remains within the Mid Holocene variability range (ca. + 2 °C compared to the 20th century, Heiri et al., 2015; Finsinger et al., 2019). However, if intense forestry should

decline, e.g. as a consequence of nature protection measures, more diverse forests may re-establish. If climate should become > 2° C warmer, possibly causing a reduction of moisture availability (Kovats et al, 2014; Henne et al. 2018), drought-sensitive beech may rapidly decline, giving way to unprecedented forest communities that will likely include drought-resistant deciduous species such as *Quercus pubescens*, drought-resistant evergreen broadleaved species such as *Quercus ilex* and warm-temperate conifers such as *Abies alba* (Bugmann et al., 2015; Henne et al., 2015; Henne et al., 2018).

6 Conclusions

We present a novel highly-resolved vegetation and fire history record from Central Europe that covers the entire post-LGM period. Radiocarbon dating on terrestrial plant remains (i.e. *Salix herbacea* leaf) resulted in a calibrated age of ca. 19,200 cal BP (18,890–19,520 cal BP, 95 % (2σ) probabilities) for the bottom of the sediment sequence. To our knowledge, together with the novel radiocarbon date from the bottom sediments of Lago di Monate of 19,300 cal BP (18,780–19,930 cal BP, 95 % (2σ) probabilities, ~~see~~ Table 2), this date provides the oldest age coming from peri-alpine lakes that were created by deglaciation after the ice collapse at the end of the LGM. Deglaciation was followed by the rapid establishment of pioneer steppe vegetation. After HE-1 (end ca. 16,700 cal BP, Stanford et al., 2011) shrubs (*Betula nana*, *Juniperus*, *Salix*) and probably trees (likely *Betula pubescens*, *Betula pendula*) expanded, which is comparable to recent ecosystem changes in the Arctic in response to ongoing global warming (Pearson et al., 2013, Brugger et al., 2019). Starting points of important vegetation reorganizations at 16,000, 14,600, 11,600 and 8200 cal BP were strongly linked to climate change (temperature and/ or precipitation shifts). No apparent inertia nor lags of population establishments were detected, implying a very high sensitivity and adjustment capacity of plant communities to climatic and environmental changes at decadal scales. These rapid responses without any apparent lags (due to e.g. migration) are explained by the very efficient distribution mechanisms of plants (e.g. winged fruits or bird transport of acorns, ~~see~~ Firbas, 1949, Tinner and Lotter, 2006) and the proximity to the refugia (< 400 km) of temperate and boreal species (Kaltenrieder et al., 2009, Samartin et al., 2012, Gubler et al., 2018). The onset of varved sediments (7000 cal BP) was closely related to vegetation opening for land use. Land use gradually overrode climate as the dominant factor in determining vegetation composition and structure during the Late Holocene. Present-day beech forests have been shaped by anthropogenic disturbances over millennia and were resilient to Mid and Late Holocene climate change. However, recent climate warming may exceed the Mid and Late Holocene climate variability releasing sudden collapses and unprecedented reorganizations of Central European ecosystems.

Data availability

The complete pollen and microscopic charcoal data sets are available through the Neotoma Palaeoecology Database (https://www.neotomadb.org). Pollen: http://dx.doi.org/10.21233/6N58-K786 (Rey et al., 2020a); Microscopic charcoal: http://dx.doi.org/10.21233/XD5R-PF83 (Rey et al., 2020b).

Author contributions

F.R. carried out all pollen and most of the quantitative analyses, constructed the chronology, arranged all figures and led the writing. E.G. initially designed the research project and helped with interpreting the data sets. C.S. calculated the zonation and gave important scientific inputs. A.H. obtained funding and contributed with the

discussion of local and regional archaeology. S.S. was responsible for radiocarbon dating. W.T. helped designing the research project, received funding and wrote major parts of the manuscript. All authors contributed and commended critically on the manuscript and gave final approval for publication.

Competing interests

The authors declare that they have no conflict of interest.

Acknowledgements

We thank Willi Tanner, Julia Rhiner, Sandra O. Brügger, Stéphanie Samartin, Lena Thöle and Petra Beffa for their valuable help during the corings, Edith Vogel for executing the radiocarbon dating, André F. Lotter for his important inputs into the analysis of varved lake sediments, Stamatina Makri and Julian Laabs for helping with the maps, Werner E. Stöckli for providing the idea of gaining oldest bottom lake sediment dates, Adriano Boschetti and the Beyond Lake Villages (BeLaVi) project team for constructive discussions, Jacqueline van Leeuwen for double checking some pollen identifications and César Morales del Molino for his help with archiving the data sets. We are grateful to the editor Nathalie Combourieu-Nebout and three anonymous reviewers for their valuable comments on previous versions of the manuscript.

Financial support

This research study has been supported by the Swiss National Science Foundation (SNF 200021_149203/1).

References

Adolf, C., Wunderle, C., Colombaroli, C., Weber, H., Gobet, E., Heiri, O., van Leeuwen, J. F. N., Bigler, C., Connor, S. E., Gałka, M., La Mantia, T., Makhortykh, S., Svitavská-Svobodová, H., Vannière, B., and Tinner, W.: The sedimentary and remote-sensing reflection of biomass burning in Europe, Glob. Ecol. Biogeogr., 27, 199–212, https://doi.org/10.1111/geb.12682, 2018.

Ammann, B.: Late-Quaternary palynology at Lobsigensee – Regional vegetation history and local lake development, Diss. Bot., 137, 1–157, 1989.

Ammann, B., and Tobolski, K.: Vegetational development during the Late-Würm at Lobsigensee (Swiss Plateau). Studies in the late Quaternary of Lobsigensee 1, Rev. Paléobiol. 2, 163–180, 1983.

Ammann, B., van Leeuwen, J. F. N., van der Knaap, W. O., Lischke, H., Heiri, O., and Tinner, W.: Vegetation responses to rapid warming and to minor climatic fluctuations during the Late-Glacial Interstadial (GI-1) at Gerzensee (Switzerland), Palaeogeogr., Palaeoclimatol., Palaeoecol., http://dx.doi.org/10.1016/j.palaeo.2012.07.010, 2013.

Beckmann, M.: Pollenanalytische Untersuchung der Zeit der Jäger und Sammler und der ersten Bauern an zwei Lokalitäten des Zentralen Schweizer Mittellandes, Diss. Bot., 390, 1–223, 2004.

Bennett, K. D.: Determination of the number of zones in a biostratigraphical sequence, New Phytol., 132, 155–170, https://doi.org/10.1111/j.1469-8137.1996.tb04521.x, 1996.

Berger, A., and Loutre, M. F.: Insolation values for the climate of the last 10 million years, Quat. Sci. Rev., 10, 297–317, https://doi.org/10.1016/0277-3791(91)90033-Q, 1991.

Beug, H.-J. (Ed.): Leitfaden der Pollenbestimmung für Mitteleuropa und angrenzende Gebiete, Pfeil, Munich, Germany, 2004.

Bini, A., Buoncristiani, J.-F., Couterrand, S., Ellwanger, D., Felber, M., Florineth, D., Graf, H. R., Keller, O., Kelly, M, Schlüchter, C., and Schoeneich, P.: Die Schweiz während des letzteiszeitlichen Maximums (LGM) 1:500000, Bundesamt für Landestopographie swisstopo, 2009.

Birks, H. H., and Ammann, B.: Two terrestrial records of rapid climatic change during the Glacial–Holocene transition (14,000–9,000 calendar years BP) from Europe. Proc. Natl. Acad. Sci. U.S.A., 97, 1390–1394, https://doi.org/10.1073/pnas.97.4.1390, 2000.

Birks, H. J. B.: The identification of Betula nana pollen, New Phytol., 67, 309–314, https://doi.org/10.1111/j.1469-8137.1968.tb06386.x, 1968.

Birks, H. J. B., and Gordon, A. D. (Eds.): Numerical Methods in Quaternary Pollen Analysis, Academic Press, London, UK, 1985.

Birks, H. J. B., and Line, J. M.: The use of rarefaction analysis for estimating palynological richness from quaternary pollen-analytical data, Holocene, 2, 1–10, https://doi.org/10.1177/095968369200200101, 1992.

Birks, H. J. B., and Tinner, W.: European tree dynamics and invasions during the Quaternary, in: Introduced tree species in European forests: opportunities and challenges, edited by: Krumm, F., and Vítková, L., European Forest Institute, Freiburg, Germany, 22–43, 2016.

Birks, H. J. B., Felde, V. A., Bjune, A. E., Grytnes, J.-A., Seppä, H., and Giesecke T.: Does pollen-assemblage richness reflect floristic richness? A review of recent developments and future challenges, Rev. Palaeobot. Palynol., 228, 1–25, http://dx.doi.org/10.1016/j.revpalbo.2015.12.011, 2016.

Birks, H. J. B., Birks, H. H., and Ammann, B.: The fourth dimension of vegetation, Science, 354, 412–413, https://doi.org/10.1126/science.aai8737, 2016.

Blaauw, M.: Methods and code for 'classical' age-modelling of radiocarbon sequences, Quat. Geochronol., 5, 512–518, https://doi.org/10.1016/j.quageo.2010.01.002, 2010.

Bronk Ramsey, C.: Analysis of chronological information and radiocarbon calibration: the program OxCal, Archaeol. Comput. Newsl., 41, 11–16, 1994.

Bronk Ramsey, C.: Radiocarbon calibration and analysis of stratigraphy: the OxCal program, Radiocarbon, 37, 425–430, https://doi.org/10.1017/S0033822200030903, 1995.

Bronk Ramsey, C.: Development of the radiocarbon calibration program OxCal, Radiocarbon, 43, 355–363, https://doi.org/10.1017/S0033822200038212, 2001.

Bronk Ramsey, C., van der Plicht, J., and Weninger, B.: 'Wiggle matching' radiocarbon dates, Radiocarbon, 43, 381–389, https://doi.org/10.1017/S0033822200038248, 2001.

Brugger, S. O., Gobet, E., Blunier, T., Morales-Molino, C., Lotter, A. F., Fischer, H., Schwikowski, M., and Tinner, W.: Palynological insights into global change impacts on Arctic vegetation, fire, and pollution recorded in Central Greenland ice, Holocene 29, 1189–1197, https://doi.org/10.1177/0959683619838039, 2019.

Bugmann, H., Brang, P., Elkin, C., Henne, P. D., Jakoby, O., Lévesque, M., Lischke, H., Psomas, A., Rigling, A., Wermelinger, B., and Zimmermann, N. E.: Climate change impacts on tree species, forest properties, and ecosystem services, in: CH2014-impacts, toward quantitative scenarios of climate change impacts in

Switzerland, edited by: Raible C. C., and Strassmann, K. M., 79–88, Bern, Switzerland: OCCR, FOEN, MeteoSwiss, C2SM, Agroscope, ProClim, Bern, Switzerland, 2015.

Bullinger, J., Lämmli, M., and Leuzinger-Piccand, C.: Le site magdalénien de plein air de Moosbühl: nouveaux éléments de datation et essai d'interprétation des données spatiales, Jahrb. Schweiz. Ges. Ur- Frühgesch., 80, 7–26, 1997.

Clark, J. S., Merkt, J., and Müller, H.: Post-glacial fire, vegetation and human history on the northern alpine forelands, South-Western Germany, J. Ecol., 77, 897–925, 1989.

Clegg, B. F., Tinner, W., Gavin, D. G., and Hu, F. S.: Morphological differentiation of Betula (birch) pollen in northwest North America and its palaeoecological application, Holocene, 16, 791–803, https://doi.org/10.1191/0959683605hl788rp, 2005.

Colombaroli, D., and Tinner, W.: Determining the long-term changes in biodiversity and provisioning services along a transect from Central Europe to the Mediterranean, Holocene, 23, 1625–1634, https://doi.org/10.1177/0959683613496290, 2013.

Conedera, M., Krebs, P., Tinner, W., Pradella, M., and Torriani, D.: The cultivation of Castanea sativa (Mill.) in Europe, from its origin to its diffusion on a continentalscale, Veg. Hist. and Archaeobot., 13, 161–179, https://doi.org/10.1007/s00334-004-0038-7, 2004.

Conedera, M., Tinner, W., Crameri, S., Torriani, D., and Herold, A.: Taxon-related pollen source areas for lake basins in the southern Alps: an empirical approach, Veg. Hist. Archaeobot., 15, 263–272, https://doi.org/10.1007/s00334-006-0056-8, 2006.

Cupillard, C., Magny, M., Bocherens, H., Bridault, A., Bégeot, C., Bichet, V., Bossuet, G., Drucker, D. G., Gauthier, E., Jouannic, G., Millet, L., Richard, H., Rius, D., Ruffaldi, P., and Walter-Simonnet, A.-V.: Changes in ecosystems, climate and societies in the Jura Mountains between 40 and 8 ka cal BP, Quat. Int., 378, 40–72, http://dx.doi.org/10.1016/j.quaint.2014.05.032, 2015.

de Beaulieu, J.-L., and Reille, M.: A long Upper Pleistocene pollen record from Les Echets, near Lyon, France, Boreas, 13, 111–132, 1984.

de Beaulieu, J.-L., and Reille, M.: The last climatic cycle at La Grande Pile (Vosges, France). A new profile, Quat. Sci. Rev., 11, 431–438, 1992.

Duprat-Oualid, F., Rius, D., Bégeot, C., Magny, M., Millet, L., Wulf, S., and Appelt, O.: Vegetation response to abrupt climate changes in Western Europe from 45 to 14.7k cal a BP: the Bergsee lacustrine record (Black Forest, Germany), J. Quat. Sci., 32, 1008–1021, https://doi.org/10.1002/jqs.2972, 2017.

Ebnöther, C., and Wyss, S.: Brenodor – Brenodurum im Brennpunkt: Fakten, Fragen und Perspektiven – Zu den Ergebnissen der Sondierungen von 2000 im Vicus Reichenbachwald (Bern-Engehalbinsel), Jahrb. Schweiz. Ges. Ur- Frühgesch., 87, 282–296, 2004.

Ehlers, J., and Gibbard, P. L. (Eds.): Quaternary Glaciations – Extent and Chronology: Part I: Europe, Elsevier, Amsterdam, The Netherlands, 2004.

Ehlers, J., Gibbard, P. L., and Hughes, P. D. (Eds.): Quaternary Glaciations – Extent and Chronology: A Closer Look, Elsevier, Amsterdam, The Netherlands, 2011.

Finsinger, W., and Tinner, W.: Minimum count sums for charcoal concentration estimates in pollen slides: accuracy and potential errors, Holocene, 15, 293–297, https://doi.org/10.1191/0959683605hl808rr, 2005.

Finsinger, W., Tinner, W., van der Knaap, W. O., and Ammann, B.: The expansion of hazel (Corylus avellana L.) in the southern Alps: a key for understanding its early Holocene history in Europe?, Quaternary Sci. Rev., 25, 612–631, https://doi.org/10.1016/j.quascirev.2005.05.006, 2006.

Finsinger, W., Schwörer, C., Heiri, O., Morales-Molino, C., Ribolini, A., Giesecke, T., Haas, J. N., Kaltenrieder, P., Magyari, E. K., Ravazzi, C., Rubiales, J. M., and Tinner, W.: Fire on ice and frozen trees? Inappropriate radiocarbon dating lead to unrealistic reconstructions, New Phytol., 222, 657–662, https://doi.org/10.1111/nph.15354, 2019.

Firbas, F. (Ed.): Spät- und nacheiszeitliche Waldgeschichte Mitteleuropas nördlich der Alpen, Fischer, Jena, Germany, 1949.

Fleitmann, D., Cheng, H., Badertscher, S., Edwards, R. L., Mudelsee, M., Göktürk, O. M., Fankhauser, A., Pickering, R., Raible, C. C., Matter, A., Kramers, J., and Tüysüz, O.: Timing and climatic impact of Greenland interstadials recorded in stalagmites from northern Turkey, Geophys. Res. Lett., 36, L19707, https://doi.org/10.1029/2009GL040050, 2009.

Gill, J. L., McLauchlan, K. K., Skibbe, A. M., Goring, S., Zirbel, C. R., and Williams, J. W.: Linking abundances of the dung fungus Sporormiella to the density of bison: implications for assessing grazing by megaherbivores in palaeorecords, J. Ecol., 101, 1125–1136, https://doi.org/10.1111/1365-2745.12130, 2013.

Gobet, E., Tinner, W., Hubschmid, P., Jansen, I., Wehrli, M., Ammann, B., and Wick, L.: Influence of human impact and bedrock differences on the vegetational history of the Insubrian Southern Alps, Veg. Hist. Archaeobot, 9, 175–178, https://doi.org/10.1007/BF01299802, 2000.

Gubler, M., Henne, P. D., Schwörer, C., Boltshauser-Kaltenrieder, P., Lotter, A. F., Brönnimann, S., and Tinner, W.: Microclimatic gradients provide evidence for a glacial refugium for temperate trees in a sheltered hilly landscape of Northern Italy, J. Biogeogr., 45, 2564–2575, https://doi.org/10.1111/jbi.13426, 2018.

Guthruf, J., Zeh, M., and Guthruf-Seiler, K. (Eds.): Kleinseen im Kanton Bern, Haupt, Bern, Switzerland, pp. 138–141, 1999.

Hadorn, P.: Vegetationsgeschichtliche Studie am Nordufer des Lac de Neuchâtel: Pollenanalytische Untersuchungen im Loclat, in der Bucht von Hauterive/Saint-Blaise und in den neolithischen Ufersiedlungen von Saint-Blaise/Bain des Dames, Ph.D. thesis, University of Bern, Switzerland, 112 pp., 1992.

Hafner, A., Harb, C., Amstutz, M., Francuz, J., and Moll-Dau, F.: Moosseedorf, Moossee Oststation, Strandbad – Strandbadneubau, Pfahlbauten und das älteste Boot der Schweiz, Jahrbuch des Archäologischen Dienstes des Kantons Bern, ArchBE 2012, 71–77, http://doi.org/10.5169/seals-726587, 2012.

Hajdas, I., Ivy, S. D., Beer, J., Bonani, G., Imboden, D., Lotter, A. F., Sturm, M., and Suter, M.: AMS radiocarbon dating and varve chronology of Lake Soppensee: 6000 to 12000 ^{14}C years BP, Clim. Dyn., 9, 107–116, https://doi.org/10.1007/BF00209748, 1993.

Harb, C. (Ed.): Moosseedorf, Moossee – Ein Überblick über 160 Jahre Pfahlbauforschung, Archäologischer Dienst des Kantons Bern, Bern, Switzerland, 2017.

Heegaard, E., Birks, H. J. B., and Telford, R. J.: Relationships between calibrated ages and depth in stratigraphical sequences: an estimation procedure by mixed-effect regression, Holocene, 15, 612–618, https://doi.org/10.1191/0959683605hl836rr, 2005.

Heiri, O., and Millet, L.: Reconstruction of late glacial summer temperatures from chironomid assemblages in Lac Lautrey (Jura, France), J. Quat. Sci., 20, 33–44, https://doi.org/10.1002/jqs.895, 2005.

Heiri, O., Brooks, S. J., Renssen, H., Bedford, A., Hazekamp, M., Ilyashuk, B., Jeffers, E. S., Lang, B., Kirilova, E., Kuiper, S., Millet, L., Samartin, S., Tóth, M., Verbruggen, F., Watson, J. E., van Ash, N., Lammertsma, E., Amon, L., Birks, H. H., Birks, H. J. B., Mortensen, M. F., Hoek, W. Z., Magyari, E., Sobrino, C. M., Seppä, H., Tinner, W., Tonkov, S., Veski, S., and Lotter, A. F.: Validation of climate model-inferred regional temperature change for late-glacial Europe, Nat. Commun., 5:4914, https://doi.org/10.1038/ncomms5914, 2014.

Heiri, O., Ilyashuk, B., Millet, L., Samartin, S., and Lotter A. F.: Stacking of discontinuous regional palaeoclimate records: Chironomid-based summer temperatures from the Alpine region, Holocene 25, 137–149, https://doi.org/10.1177/0959683614556382, 2015.

Henne, P. D., Elkin, C. M., Reineking, B., Bugmann, H., and Tinner, W.: Did soil development limit spruce (Picea abies) expansion in the Central Alps during the Holocene? Testing a palaeobotanical hypothesis with a dynamic landscape model, J. Biogeogr., 38, 933–949, https://doi.org/10.1111/j.1365-2699.2010.02460.x, 2011.

Henne, P. D., Elkin, C., Franke, J., Colombaroli, D., Calò, C., La Mantia, T., and Tinner, W.: Reviving extinct Mediterranean forests increases ecosystem potential in a warmer future, Front. Ecol. Environ., 13, 356–362, https://doi.org/10.1890/150027, 2015.

Henne, P. D., Bigalke, M., Büntgen, U., Colombaroli, D., Conedera, M., Feller, U., and Tinner, W.: An empirical perspective for understanding climate change impacts in Switzerland, Reg. Environ. Chang., 18, 205–221, https://doi.org/10.1007/s10113-017-1182-9, 2018.

Hofer, P., and Meyer, H. J. (Eds.): Die Burg Nydegg: Forschungen zur frühen Geschichte von Bern, Haupt, Bern, 1991.

Hofstetter, S., Tinner, W., Valsecchi, V., Carraro, G., and Conedera, M.: Lateglacial and Holocene vegetation history in the Insubrian Southern Alps – New indications from a small-scale site, Veg. Hist. Archaeobot., 15, 87–98, https://doi.org/10.1007/s00334-005-0005-y, 2006.

Hughes, P. D., Gibbard, P. L., and Ehlers, J.: Timing of glaciation during the last glacial cycle: evaluating the concept of a global 'Last Glacial Maximum' (LGM), Earth-Sci. Rev., 125, 171–198, https://doi.org/10.1016/j.earscirev.2013.07.003, 2013.

Hurlbert, S. H.: The nonconcept of species diversity: a critique and alternative parameters, Ecology, 52, 577–586, https://doi.org/10.2307/1934145, 1971.

Ilyashuk, B., Gobet, E., Heiri, O., Lotter, A. F., van Leeuwen, J. F. N., van der Knaap, W. O., Ilyashuk, E., Oberli, F., Ammann, B.: Lateglacial environmental and climatic changes at the Maloja Pass, Central Swiss Alps, as recorded by chironomids and pollen, Quat. Sci. Rev., 28, 1340–1353, https://doi.org/10.1016/j.quascirev.2009.01.007, 2009.

Joannin, S., Vannière, B., Galop, D., Peyron, O., Haas, J. N., Gilli, A., Chapron, E., Wirth, S. B., Anselmetti, F., Desmet, M., and Magny, M.: Climate and vegetation changes during the Lateglacial and early–middle Holocene at Lake Ledro (southern Alps, Italy), Clim. Past, 9, 913–933, http://doi.org/10.5194/cp-9-913-2013, 2013.

Kaltenrieder, P., Belis, C. A., Hofstetter, S., Ammann, B., Ravazzi, C., and Tinner, W.: Environmental and climatic conditions at a potential Glacial refugial site of tree species near the Southern Alpine glaciers. New insights from multiproxy sedimentary studies at Lago della Costa (Euganean Hills, Northeastern Italy), Quaternary Sci. Rev., 28, 2647–2662, https://doi.org/10.1016/j.quascirev.2009.05.025, 2009.

Kleinmann, A., Merkt, J., and Müller, H.: Sedimente des Degersees: Ein Umweltarchiv – Sedimentologie und Palynologie, in: Pfahlbausiedlungen am Degersee – Archäologische und naturwissenschaftliche Untersuchungen, edited by: Mainberger, M., Merkt, J., and Kleinmann, A., Theiss, Darmstadt, Germany, 409–471, 2015.

Kovats, R. S., Valentini, R., Bouwer, L. M., Georgopoulou, E., Jacob, D., Martin, E., and Soussana, J.-F.: Europe, in: Climate change 2014 – Impacts, adaptation, and vulnerability. Part B: Regional aspects. Contribution of Working Group II to the Fifth Assessment Report of the Intergovernmental Panel on Climate Change, edited by: Barros, V. R., Field, C. B., Dokken, D. J., Mastrandrea, M. D., Mach, K. J., Bilir, T. E., and White, L. L., 1267–1326, Cambridge University Press, Cambridge/ New York, UK/ USA, 2014.

Lang, G. (Ed.): Quartäre Vegetationsgeschichte Europas: Methoden und Ergebnisse, Fischer, Jena, Germany, 1994.

Larocque, I., and Finsinger, W.: Late-glacial chironomid-based temperature reconstructions for Lago Piccolo di Avigliana in the southwestern Alps (Italy), Palaeogeogr. Palaeoclimatol. Palaeoecol., 257, 207–223, https://doi.org/10.1016/j.palaeo.2007.10.021, 2008.

Lauber, K., Wagner, G., and Gygax, A. (Eds.): Flora helvetica, 5th edition, Haupt, Bern, Switzerland, 2014.

Lauterbach, S., Chapron, E., Brauer, A., Hüls, M., Gilli, A., Arnaud, F., Piccin, A., Nomade, J., Desmet, M., von Grafenstein, U., and DecLakes Participants: A sedimentary record of Holocene surface runoff events and earthquake activity from Lake Iseo (Southern Alps, Italy), Holocene, 22, 749–760, http://dx.doi.org/10.1177/0959683611430340, 2012.

Lister, G. S.: A 15,000-year isotopic record from Lake Zürich of deglaciation and climatic change in Switzerland, Quat. Res., 29, 129–141, http://dx.doi.org/10.1016/0033-5894(88)90056-7, 1988.

Litt, T., Schölzel, C., Kühl, N., and Brauer, A.: Vegetation and climate history in the Westeifel Volcanic Field (Germany) during the past 11000 years based on annually laminated lacustrine maar sediments, Boreas, 38, 679–690, https://doi.org/10.1111/j.1502-3885.2009.00096.x, 2009.

Livingstone, D. M., and Lotter, A.F.: The relationship between air and water temperatures in lakes of the Swiss Plateau: a case study with palæolimnological implications, J. Paleolimnol., 19, 181–198, https://doi.org/10.1023/A:1007904817619, 1998.

Lotter, A. F.: Late-glacial and Holocene vegetation history and dynamics as shown by pollen and plant macrofossil analyses in annually laminated sediments from Soppensee, central Switzerland, Veg. Hist. Archaeobot., 8, 165–184, https://doi.org/10.1007/BF02342718, 1999.

Lotter, A. F., and Kienast, F.: Validation of a forest succession model by means of annually laminated sediments. Geol. Surv. Finland, 14, 25–31, 1992.

Lotter, A. F., and Zbinden, H.: Late-Glacial pollen analysis, oxygen-isotope record, and radiocarbon stratigraphy from Rotsee (Lucerne), Central Swiss Plateau, Eclogae Geol. Helv., 82, 191–202, 1989.

Lotter, A. F., Birks, H. J. B., Eicher, U., Hofmann, W., Schwander, J., and Wick, L.: Younger Dryas and Allerød summer temperatures at Gerzensee (Switzerland) inferred from fossil pollen and cladoceran assemblages, Palaeogeogr. Palaeoclimatol. Palaeoecol., 159, 349–361, https://doi.org/10.1016/S0031-0182(00)00093-6, 2000.

Lotter, A. F., Heiri, O., Brooks, S., van Leeuwen, J. F. N., Eicher, U., and Ammann, B.: Rapid summer temperature changes during Termination 1a: high-resolution multi-proxy climate reconstructions from Gerzensee (Switzerland), Quat. Sci. Rev., 36, 103–113, https://doi.org/10.1016/j.quascirev.2010.06.022, 2012.

Lourantou, A., Lavrič, J. V., Köhler, P., Barnola, J.-M., Paillard, D., Michel, E., Raynaud, D., and Chappellaz, J.: Constraint of the CO_2 rise by new atmospheric carbon isotopic measurements during the last deglaciation, Global Biogeochem. Cy., 24, GB2015, https://doi.org/10.1029/2009GB003545, 2010.

Magny, M.: Orbital, ice-sheet, and possible solar forcing of Holocene lake-level fluctuations in west-central Europe: A comment on Bleicher, Holocene, 23, 1202–1212, https://doi.org/10.1177/0959683613483627, 2013.

Magny, M., Bossuet, G., Ruffaldi, P., Leroux, A., and Mouthon, J.: Orbital imprint on Holocene palaeohydrological variations in west-central Europe as reflected by lake-level changes at Cerin (Jura Mountains, eastern France), J. Quat. Sci. 26, 171–177, https://doi.org/10.1002/jqs.1436, 2011.

Magny, M., Joannin, S., Galop, D., Vannière, B., Haas, J. N., Bassetti, M., Bellintani, P., Scandolari, R., and Desmet, M.: Holocene palaeohydrological changes in the northern Mediterranean borderlands as reflected by the lake-level record of Lake Ledro, northeastern Italy, Quat. Res., 77, 382–396, https://doi.org/10.1016/j.yqres.2012.01.005, 2012.

Marta, S., Mattoccia, M., and Sbordoni, V.: Modelling landscape dynamics in a glacial refugium – or the spatial and temporal fluctuations of tree line altitudes, J. Biogeogr., 40, 1767–1779, https://doi.org/10.1111/jbi.12120, 2013.

MeteoSwiss: Klimadiagramme und Normwerte pro Station, Federal Office of Meteorology and Climatology MeteoSwiss, Zurich-Airport, Switzerland, 2017.

Monegato, G., Ravazzi, C., Donegana, M., Pini, R., Calderoni, G., and Wick, L.: Evidence of a two-fold glacial advance during the last glacial maximum in the Tagliamento end moraine system (eastern Alps), Quat. Res., 68, 284–302, https://doi.org/10.1016/j.yqres.2007.07.002, 2007.

Moore, P. D., Webb, J. A., and Collison, M. E. (Eds.): Pollen Analysis, Blackwell Scientific Publications, Oxford, UK, 1991.

Nielsen, E.: Response of the Lateglacial fauna to climatic change, Palaeogeogr. Palaeoclimatol. Palaeoecol., 391, 99–110, https://doi.org/10.1016/j.palaeo.2012.12.012, 2013.

Nielsen, E. (Ed.): Die späteiszeitliche Fundstelle Moosseedorf, Moosbühl 1, Archäologischer Dienst des Kantons Bern, Bern, Switzerland, 2018.

North Greenland Ice Core Project members: High resolution record of Northern Hemisphere climate extending into the last interglacial period, Nature, 431, 147–151, https://doi.org/10.1038/nature02805, 2004.

Odgaard, B. V.: Fossil pollen as a record of past biodiversity, J. Biogeogr., 26, 7–17, https://doi.org/10.1046/j.1365-2699.1999.00280.x, 1999.

Pearson, R. G., Phillips, S. J., Loranty, M. M., Beck, P. S. A., Damoulas, T., Knight, S. J., and Goetz, S. J.: Shifts in Arctic vegetation and associated feedbacks under climate change, Nat. Clim. Chang., 3, 673–677, https://doi.org/10.1038/nclimate1858, 2013.

Pini, R.: A high-resolution Late-glacial–Holocene pollen diagram from Pian di Gembro (Central Alps, Northern Italy), Veget. Hist. Archaeobot., 11, 251–262, https://doi.org/10.1007/s003340200038, 2002.

Pini, R., Ravazzi, C., Aceti, A., Castellano, L., Perego, R., Quirino, T., and Vallè, F.: Ecological changes and human interaction in Valcamonica, the rock art valley, since the last deglaciation, Alpine Mediterr. Quat., 29, 19–34, 2016.

R Development Core Team: R: a language and environment for statistical computing. Vienna, Austria: R Foundation for Statistical Computing, Vienna, Austria, 2018.

Ranalli, P., and Venturi, G.: Hemp as a raw material for industrial applications, Euphytica, 140, 1–6, https://doi.org/10.1007/s10681-004-4749-8, 2004.

Ravazzi, C., Pini, R., Badino, F., De Amicis, M., Londeix, L., and Reimer, P.J.: The latest LGM culmination of the Garda Glacier (Italian Alps) and the onset of glacial termination. Age of glacial collapse and vegetation chronosequence, Quat. Sci. Rev., 105, 26–47, http://dx.doi.org/10.1016/j.quascirev.2014.09.014, 2014.

Reille, M. (Ed.): Pollen et spores d'Europe et d'Afrique du Nord, Laboratoire de botanique historique et palynology, Marseille, France, 1992.

Reimer, P. J., Bard, E., Bayliss, A., Beck, J. W., Blackwell, P. G., Bronk Ramsey, C., Buck, C. E., Cheng, H., Edwards, R. L., Friedrich, M., Grootes, P. M., Guilderson, T. P., Haflidason, H., Hajdas, I., Hatté, C., Heaton, T. J., Hoffmann, D. L., Hogg, A. G., Hughen, K. A., Kaiser, K. F., Kromer, B., Manning, S. W., Niu, M., Reimer, R. W., Richards, D. A., Scott, E. M., Southon, J. R., Staff, R. A., Turney, C. S. M., and van der Plicht, J.: IntCal13 and Marine13 radiocarbon age calibration curves 0–50,000 years cal BP, Radiocarbon, 55, 1869–87, https://doi.org/10.2458/azu_js_rc.55.16947, 2013.

Rey, F., Schwörer, C., Gobet, E., Colombaroli, D., van Leeuwen, J. F. N., Schleiss, S., and Tinner, W.: Climatic and human impacts on mountain vegetation at Lauenensee (Bernese Alps, Switzerland) during the last 14,000 years, Holocene, 23, 1415–1427, https://doi.org/10.1177/0959683613489585, 2013.

Rey, F., Gobet, E., van Leeuwen, J. F. N., Gilli, A., van Raden, U. J., Hafner, A., Wey, O., Rhiner, J., Schmocker, D., Zünd, J., and Tinner, W.: Vegetational and agricultural dynamics at Burgäschisee (Swiss Plateau) recorded for 18,700 years by multi-proxy evidence from partly varved sediments, Veg. Hist. Archaeobot., 26, 571–586. https://doi.org/10.1007/s00334-017-0635-x, 2017.

Rey, F., Gobet, E., Schwörer, C., Wey, O., Hafner, A., and Tinner, W.: Causes and mechanisms of synchronous succession trajectories in primeval Central European mixed Fagus sylvatica forests, J. Ecol., 107, 1392–1408, https://doi.org/10.1111/1365-2745.13121, 2019a.

Rey, F., Gobet, E., Szidat, S., Lotter, A. F., Gilli, A., Hafner, A., and Tinner, W.: Radiocarbon wiggle matching on laminated sediments delivers high-precision chronologies, Radiocarbon, 61, 265–285, https://doi.org/10.1017/rdc.2018.47, 2019b.

Rey, F., Gobet, E., Schwörer, C., Hafner, A., Szidat, S., and Tinner, W.: Climate impacts on vegetation and fire dynamics since the Last Glacial Maximum at Moossee (Switzerland), Neotoma Palaeoecology Database, http://dx.doi.org/10.21233/6N58-K786, 2020a.

Rey, F., Gobet, E., Schwörer, C., Hafner, A., Szidat, S., and Tinner, W.: Climate impacts on vegetation and fire dynamics since the Last Glacial Maximum at Moossee (Switzerland), Neotoma Palaeoecology Database, http://dx.doi.org/10.21233/XD5R-PF83, 2020b.

Samartin, S., Heiri, O., Lotter, A. F., and Tinner, W.: Climate warming and vegetation response after Heinrich event 1 (16,700–16,000 cal yr BP) in Europe south of the Alps, Clim. Past, 8, 1913–1927, https://doi.org/10.5194/cp-8-1913-2012, 2012.

Samartin, S., Heiri, O., Kaltenrieder, P., Kühl, N., and Tinner, W.: Reconstruction of full glacial environments and summer temperatures from Lago della Costa, a refugial site in Northern Italy, Quat. Sci. Rev., 143, 107–119, https://doi.org/10.1016/j.quascirev.2016.04.005, 2016.

Schmid, S. M., Fügenschuh, B., Kissling, E., and Schuster, R.: Tectonic map and overall architecture of the Alpine orogeny, Eclogae Geol. Helv., 97, 93–117, https://doi.org/10.1007/s00015-004-1113-x, 2004.

Schumacher, S., and Bugmann, H.: The relative importance of climatic effects, wildfires and management for future forest landscape dynamics in the Swiss Alps, Glob. Chang. Biol., 12, 1435–1450, https://doi.org/10.1111/j.1365-2486.2006.01188.x, 2006.

Schwander, J., Eicher, U., and Ammann, B.: Oxygen isotopes of lake marl at Gerzensee and Leysin (Switzerland), covering the Younger Dryas and two minor oscillations, and their correlation to the GRIP ice core, Palaeogeogr., Palaeoclimatol., Palaeoecol., 159, 203–214, https://doi.org/10.1016/S0031-0182(00)00085-7, 2000.

Schwörer, C., Henne, P. D., and Tinner, W.: A model-data comparison of Holocene timberline changes in the Swiss Alps reveals past and future drivers of mountain forest dynamics. Glob. Chang. Biol., 20, 1512–1526, https://doi.org/10.1111/gcb.12456, 2014.

Schwörer, C., Colombaroli, D., Kaltenrieder, P., Rey, F., and Tinner, W.: Early human impact (5,000–3,000 BC) affects mountain forest dynamics in the Alps, J. Ecol., 103, 281–295, https://doi.org/10.1111/1365-2745.12354, 2015.

Seguinot, J., Ivy-Ochs, S., Jouvet, G., Huss, M.,Funk, M., and Preusser, F.: Modelling last glacial cycle ice dynamics in the Alps. Cryosphere, 12, 3265–3285, https://doi.org/10.5194/tc-12-3265-2018, 2018.

Šmilauer, P., and Lepš, J. (Eds.) Multivariate Analysis of Ecological Data using CANOCO 5, Cambridge University Press, Cambridge, UK, doi:10.1017/CBO9781139627061, 2014.

Stanford, J. D., Rohling, E. J., Bacon, S., Roberts, A. P., Grousset, F. E., and Bolshaw, M.: A new concept for the paleoceanographic evolution of Heinrich event 1 in the North Atlantic, Quaternary Sci. Rev., 30, 1047–1066, https://doi.org/10.1016/j.quascirev.2011.02.003, 2011.

Steinhilber, F., Beer, J., and Fröhlich, C.: Total solar irradiance during the Holocene, Geophys. Res. Lett., 36, L19704, https://doi.org/10.1029/2009GL040142, 2009.

Stockmarr, J.: Tablets with spores used in absolute pollen analysis, Pollen Spores, 13, 615–621, 1971.

Stuiver, M., and Polach, H. A.: Discussion – Reporting of ^{14}C data, Radiocarbon, 19, 355–363, https://doi.org/10.1017/S0033822200003672, 1977.

Stuiver, M., and Reimer, P.: Extended ^{14}C data base and revised CALIB 3.0 ^{14}C age calibration program, Radiocarbon, 35, 215–230, https://doi.org/10.1017/S0033822200013904, 1993.

Szidat, S., Salazar, G. A., Vogel, E., Battaglia, M., Wacker, L., Synal, H.-A., and Türler, A.: ^{14}C analysis and sample preparation at the new Bern Laboratory for the Analysis of Radiocarbon with AMS (LARA), Radiocarbon 56, 561–566, https://doi.org/10.2458/56.17457, 2014.

Ter Braak, C. J. F., and Prentice, I. C.: A theory of gradient analysis. Adv. Ecol. Res., 18, 271–317, https://doi.org/10.1016/S0065-2504(03)34003-6, 1998.

Tinner, W., and Hu, F. S.: Size parameters, size-class distribution and area number relationship of microscopic charcoal: Relevance for fire reconstruction, Holocene, 13, 499–505, https://doi.org/10.1191/0959683603hl615rp, 2003.

Tinner, W., and Kaltenrieder, P.: Rapid responses of high-mountain vegetation to early Holocene environmental changes in the Swiss Alps, J. Ecol., 93, 936–947, https://doi.org/10.1111/j.1365-2745.2005.01023.x, 2005.

Tinner, W., and Lotter, A. F.: Central European vegetation response to abrupt climate change at 8.2 ka, Geology, 29, 551–554, https://doi.org/10.1130/0091-7613(2001)029<0551:CEVRTA>2.0.CO;2, 2001.

Tinner, W., and Lotter, A. F.: Holocene expansions of Fagus silvatica and Abies alba in Central Europe: where are we after eight decades of debate?, Quat. Sci. Rev., 25, 526–549, https://doi.org/10.1016/j.quascirev.2005.03.017, 2006.

Tinner, W., and Vescovi, E.: Ecologia e oscillazioni del limite degli alberi nelle Alpi dal Pleniglaciale al presente, Acta Geol., 82, 7–15, 2007.

Tinner, W., Conedera, M., Ammann, B., Gaggeler, H. W., Gedye, S., Jones, R., and Sagesser, B.: Pollen and charcoal in lake sediments compared with historically documented forest fires in southern Switzerland since AD 1920, Holocene, 8, 31–42, https://doi.org/10.1191/095968398667205430, 1998.

Tinner, W., Hubschmid, P., Wehrli, M., Ammann, B., and Conedera, M.: Long-term forest fire ecology and dynamics in southern Switzerland, J. Ecol., 87, 273–289. https://doi.org/10.1046/j.1365-2745.1999.00346.x, 1999.

Tinner, W., Lotter, A. F., Ammann, B., Conedera, M., Hubschmid, P., van Leeuwen, J. F. N., and Wehrli, M.: Climatic change and contemporaneous land-use phases north and south of the Alps 2300 BC to 800 AD, Quat. Sci. Rev., 22, 1447–1460, https://doi.org/10.1016/S0277-3791(03)00083-0, 2003.

Tinner, W., Conedera, M., Ammann, B., and Lotter, A. F.: Fire ecology north and south of the Alps since the last ice age, Holocene, 15, 1214–1226, https://doi.org/10.1191/0959683605hl892rp, 2005.

Tinner, W., Colombaroli, D., Heiri, O., Henne, P. D., Steinacher, M., Untenecker, J., Vescovi, E., Allen, J. R. M., Carraro, G., Conedera, M., Joos, F., Lotter, A. F., Luterbacher, J., Samartin, S., and Valsecchi, V.: The past ecology of Abies alba provides new perspectives on future responses of silver fir forests to global warming, Ecol. Monogr., 83, 419–439, https://doi.org/10.1890/12-2231.1, 2013.

Uglietti, C., Zapf, A., Jenk, T. M., Sigl, M., Szidat, S., Salazar, G., and Schwikowski, M.: Radiocarbon dating of glacier ice: overview, optimisation, validation and potential, Cryosphere 10, 3091–3105, https://doi.org/10.5194/tc-10-3091-2016, 2016.

van der Knaap, W. O.: Estimating pollen diversity from pollen accumulation rates: a method to assess taxonomic richness in the landscape, Holocene, 19, 159–163, https://doi.org/10.1177/0959683608098962, 2009.

van Geel, B.: Fossil ascomycetes in Quaternary deposits, Nova Hedwigia, 82, 313–329, https://doi.org/10.1127/0029-5035/2006/0082-0313, 2006.

van Geel, B., Buurman, J., Brinkkemper, O., Schelvis, J., Aptroot, A., van Reenen, G. and Hakbijl, T.: Environmental reconstruction of a Roman Period settlement site in Uitgeest (The Netherlands), with special reference to coprophilous fungi, J. Archaeol. Sci., 30, 873–883, https://doi.org/10.1016/S0305-4403(02)00265-0, 2003.

van Raden, U. J., Colombaroli, D., Gilli, A., Schwander, J., Bernasconi, S. M., van Leeuwen, J., Leuenberger, M., and Eicher, U.: High-resolution late-glacial chronology for the Gerzensee lake record (Switzerland): $\delta^{18}O$ correlation between a Gerzensee-stack and NGRIP, Palaeogeogr. Palaeoclimatol. Palaeoecol., 391, 13–24, https://doi.org/10.1016/j.palaeo.2012.05.017, 2013.

Vescovi, E., Ravazzi, C., Arpenti, E., Finsinger,W., Pini, R., Valsecchi, V., Wick, L., Ammann, B., and Tinner, W.: Interactions between climate and vegetation during the Lateglacial period as recorded by lake and mire sediment archives in Northern Italy and Southern Switzerland, Quaternary Sci. Rev., 26, 1650–1669, https://doi.org/10.1016/j.quascirev.2007.03.005, 2007.

von Büren, G. (Ed.): Der Moosseedorfsee − Neue Beiträge zur Kenntnis seiner Physiographie und Biologie mit Einbezug des Kleinen Moosseedorfsees (Hofwilsee), Haupt, Bern, Switzerland, 1943.

von Grafenstein, U., Erlenkeuser, H., Müller, J., Jouzel, J., and Johnsen, S.: The cold event 8200 years ago documented in oxygen isotope records of precipitation in Europe and Greenland, Clim. Dyn., 14, 73–81, https://doi.org/10.1007/s003820050210, 1998.

von Grafenstein, U., Erlenkeuser, H., Brauer, A., Jouzel, J., and Johnsen, S. J.: A mid- European decadal isotope-climate record from 15,500 to 5000 years BP, Science, 284, 1654–1657, https://doi.org/10.1126/science.284.5420.1654, 1999.

von Grafenstein, U., Eicher, U., Erlenkeuser, H., Ruch, P., Schwander, J., and Ammann, B.: Isotope signature of the Younger Dryas and two minor oscillations at Gerzensee (Switzerland): palaeoclimatic and palaeolimnologic interpretation based on bulk and biogenic carbonates, Palaeogeogr., Palaeoclimatol., Palaeoecol., 159, 215–229, https://doi.org/10.1016/S0031-0182(00)00086-9, 2000.

Wehrli, M., Tinner, W., and Ammann, B.: 16 000 years of vegetation and settlement history from Egelsee (Menzingen, central Switzerland), Holocene, 17, 747–761, https://doi.org/10.1177/0959683607080515, 2007.

Welten, M. (Ed.): Vegetationsgeschichtliche Untersuchungen in den westlichen Schweizer Alpen: Bern-Wallis, Denkschr. Schweiz. Natforsch. Ges., 95, 1–104, 1982.

Wick, L.: Das Hinterland von Augusta Raurica: Paläoökologische Untersuchungen zur Vegetation und Landnutzung von der Eisenzeit bis zum Mittelalter, Jahresberichte aus Augst und Kaiseraugst, 36, 209–215, 2015.

Wick, L., and Möhl, A.: The mid-Holocene extinction of silver fir (Abies alba) in the Southern Alps: a consequence of forest fires? Palaeobotanical records and forest simulations, Veg. Hist. Archaeobot., 15, 435–444, https://doi.org/10.1007/s00334-006-0051-0, 2006.

Willis, K. J., and Birks, H. J. B.: What is natural? The need for a long-term perspective in biodiversity conservation, Science, 314, 1261–1265, https://doi.org/10.1126/science.1122667, 2006.

Wirsig, C., Zasadni, J., Christl, M., Akçar, N., and Ivy-Ochs, S.: Dating the onset of LGM ice surface lowering in the High Alps, Quat. Sci. Rev., 143, 37–50, https://doi.org/10.1016/j.quascirev.2016.05.001, 2016.

Wirtz, K. W., and Lemmen, C.: A global dynamic model for the Neolithic transition, Clim. Chang., 59, 333–367, https://doi.org/10.1023/A:1024858532005, 2003.

Woillard, G. M.: Grande Pile peat bog: a continuous pollen record for the last 140,000 years, Quat. Res., 9, 1–21, 1978.

1020 **Table 1: Radiocarbon dates and calibrated ages from the Moossee record. Uncertainties of ^{14}C ages refer to 68 % probabilities (1σ) whereas ranges of calibrated and modelled ages represent 95 % probabilities (2σ).**

Lab. code	Depth (cm)	^{14}C age (BP)[a]	Age range (cal BP)[b]	Modelled age range (cal BP)[c]	Material
BE-7363.1.1	78.6−75.9	150 ± 20	5−280	-135−420	*Picea abies* needle
BE-7362.1.2	104.7−102.2	240 ± 70	5−480	-230−700	Leaf indet
BE-7361.1.1	187.5−186.3	450 ± 20	495−525	475−545	Leaf fragments indet
BE-7360.1.1	241.6−239.8	1065 ± 20	930−1050	870−1110	*Alnus glutinosa* fruit
BE-7359.1.1	261.1−259.9	1110 ± 35	935−1170	820−1285	*Alnus glutinosa* fruit
BE-7358.1.1	324.4−321.1	1495 ± 40	1305−1520	1205−1620	*Betula* fruits, *Fagus sylvatica* bud scales
BE-7357.1.1	328.0−325.1	1535 ± 30	1360−1520	1270−1600	*Betula* fruits, *Fagus sylvatica* bud scales, *Salix* bud scale, bud scale indet
BE-7356.1.1	330.8−328.6	1555 ± 40	1360−1535	1285−1625	*Betula* fruit, *Fagus sylvatica* bud scale, *Populus tremula* floral bract
BE-7355.1.1	338.5−332.2	1620 ± 40	1410−1605	1320−1700	*Betula* fruits, *Fagus sylvatica* bud scale, *Populus tremula* floral bract, *Quercus* bud scales
BE-7354.1.1	346.9−339.8	1700 ± 40	1535−1705	1450−1785	*Betula* fruits, *Populus tremula* floral bract
BE-7353.1.1	386.5−385.9	2060 ± 35	1935−2120	1840−2215	Terrestrial fruit indet
BE-7352.1.1	416.2−409.3	2290 ± 50	2150−2400	2025−2525	*Betula* fruit, *Betula* fruits scales
BE-7351.1.1	435.0−432.7	2420 ± 35	2350−2700	2655−2705	*Fagus sylvatica* bud scales
BE-7350.1.1	439.0−438.1	2630 ± 50	2540−2860	2730−2775	*Betula* fruit, *Betula* fruit scale
BE-7349.1.1	441.4−439.7	2730 ± 35	2760−2920	2765−2810	*Abies alba* bud scale, *Fagus sylvatica* bud scales, terrestrial fruit indet
BE-7348.1.1	447.0−446.4	2795 ± 40	2790−2990	2875−2920	*Fagus sylvatica* bud scale
BE-7347.1.1	449.9−448.8	2810 ± 45	2790−3055	2910−2960	*Betula* fruit, *Fagus sylvatica* bud scales
BE-7346.1.1	453.0−452.5	2900 ± 45	2890−3170	2965−3020	Bud scale indet
BE-7345.1.1	461.1−460.0	3010 ± 40	3070−3340	3085−3135	*Abies alba* bud scale, *Alnus glutinosa* bud scale, *Betula* fruits, bud scale indet, petiole indet
BE-7344.1.1	468.3−466.9	3010 ± 40	3070−3340	3185−3240	*Alnus glutinosa* fruit, *Betula* fruits, *Populus tremula* floral bract
BE-7343.1.1	472.7−472.0	3070 ± 45	3165−3380	3245−3300	*Alnus glutinosa* bud scale
BE-7342.1.1	495.8−495.0	3245 ± 50	3375−3575	3490−3550	Leaf fragments indet
BE-7341.1.1	498.0−497.3	3315 ± 40	3455−3640	3520−3580	*Abies alba* bud scale, *Fagus sylvatica* bud scale
BE-7340.1.1	500.2−499.0	3295 ± 45	3405−3635	3555−3610	*Fagus sylvatica* bud scale, terrestrial fruit indet
BE-7339.1.1	502.9−501.3	3395 ± 40	3515−3820	3585−3650	*Abies alba* bud scale, *Betula* fruit, *Fagus sylvatica* bud scales, *Quercus* bud scale, bud scale indet, terrestrial fruit indet
BE-5380.1.1	520.2−519.5	3615 ± 35	3835−4070	3840−3885	*Alnus glutinosa* fruit, terrestrial plant remain indet
BE-5631.1.1	540.3−539.8	3765 ± 40	3985−4245	4065−4105	*Alnus glutinosa* fruit, leaf fragment indet
BE-5381.1.1	543.5−543.0	3710 ± 35	3930−4150	4110−4145	*Betula* fruit, *Fagus sylvatica* bud scales
BE-5632.1.1	548.4−547.7	3865 ± 40	4155−4415	4180−4220	*Fagus sylvatica* bud scales
BE-5382.1.1	553.1−552.4	3865 ± 35	4160−4415	4270−4305	*Fagus sylvatica* bud scales
BE-5383.1.1	569.8−569.2	4190 ± 35	4590−4840	4655−4685	*Abies alba* needle, *Fagus sylvatica* bud scale
BE-5633.1.1	572.4−571.6	4160 ± 40	4570−4830	4695−4720	*Alnus glutinosa* fruit, *Betula* fruit, *Fagus sylvatica* bud scale

Table 1: ***(continued)***

Lab. code	Depth (cm)	^{14}C age (BP)[a]	Age range (cal BP)[b]	Modelled age range (cal BP)[c]	Material
BE-5384.1.1	578.7−578.3	4250 ± 20	4825−4855	4835−4860	*Populus tremula* floral bract, leaf fragments indet
BE-5385.1.1	604.6−604.0	4730 ± 20	5330−5580	5330−5360	*Alnus glutinosa* bud scale, *Alnus glutinosa* catkin, *Betula* fruits
BE-5634.1.1	606.3−605.8	4740 ± 40	5325−5585	5355−5385	*Alnus glutinosa* bud scale, *Alnus glutinosa* fruit
BE-5635.1.1	607.7−607.2	4690 ± 45	5315−5580	5395−5420	*Alnus glutinosa* bud scale, *Betula* fruit
BE-5636.1.1	612.0−611.5	4830 ± 70	5330−5720	5500−5530	*Betula* fruits, *Fagus sylvatica* bud scale
BE-5386.1.1	618.7−618.1	4970 ± 25	5615−5745	5640−5675	*Abies alba* seed, *Fagus sylvatica* bud scale, leaf fragments indet
BE-5387.1.1	624.2−623.6	5035 ± 40	5660−5900	5720−5755	*Abies alba* needle, *Abies alba* bud scale, petioles indet
BE-5388.1.1	625.9−625.2	5060 ± 35	5730−5905	5755−5790	*Alnus glutinosa* bud scale, *Betula* fruit, *Fagus sylvatica* bud scale, leaf fragments indet
BE-5637.1.1	630.8−630.3	5005 ± 50	5620−5895	5850−5885	*Betula* fruit, *Fagus sylvatica* bud scale
BE-5389.1.1	636.2−635.5	5235 ± 40	5915−6175	5965−6005	Petiole indet
BE-5638.1.1	641.3−640.8	5375 ± 40	6005−6280	6105−6140	*Alnus glutinosa* bud scale
BE-5390.1.1	646.2−645.5	5370 ± 60	6000−6285	6230−6270	*Fagus sylvatica* bud scale
BE-5639.1.1	652.7−652.1	5660 ± 45	6315−6550	6380−6420	*Fagus sylvatica* bud scales
BE-5391.1.1	656.2−655.8	5655 ± 25	6355−6495	6430−6475	*Fagus sylvatica* bud scale, bud scale indet, petioles indet
BE-5392.1.1	659.8−659.3	5760 ± 25	6490−6635	6495−6535	*Alnus glutinosa* catkin, *Alnus glutinosa* fruits
BE-5640.1.1	669.1−668.6	5875 ± 45	6565−6795	6625−6670	*Fagus sylvatica* bud scale
BE-5393.1.1	675.7−675.2	5940 ± 25	6680−6845	6740−6790	*Fagus sylvatica* bud scales, bud scales indet
BE-5394.1.1	678.3−677.8	5990 ± 40	6735−6940	6790−6845	*Fagus sylvatica* bud scale, leaf fragments indet
BE-5641.1.1	689.8−689.4	6135 ± 45	6910−7160	7010−7065	*Fagus sylvatica* bud scale, petiole indet
BE-5642.1.1	691.2−690.8	6210 ± 45	6995−7250	7035−7095	*Alnus glutinosa* fruit, *Tilia* anthers
BE-5395.1.1	767.0−765.0	7850 ± 110	8440−8990	8160−9270	Terrestrial fruit indet
BE-5396.1.1	798.0−796.0	8165 ± 25	9015−9245	8890−9370	*Tilia* fruit scale
BE-5397.1.1	867.0−865.0	9380 ± 30	10,520−10,690	10,440−10,805	*Pinus sylvestris* bud scale, *Populus tremula* floral bract, *Populus tremula* fruits, *Quercus* bud scale, *Ulmus* bud scale
BE-5398.1.1	883.0−881.0	9980 ± 60	11,250−11,710	10,960−11,890	*Betula* fruits, *Betula* fruit scales, *Pinus sylvestris* bud scales
	933.0−932.0		12,885−13,185[d]	12,740−13,350	Laacher See Tephra (LST)
BE-5399.1.1	949.0−947.0	11,675 ± 35	13,440−13,570	13,360−13,650	*Betula* fruits, *Betula* fruit scale, *Juniperus* needles
BE-5400.1.1	967.0−965.0	12,200 ± 70	13,810−14,350	13,520−14,600	*Betula* fruits, *Betula* fruit scale
BE-5401.1.1	983.0−981.0	12,350 ± 80	14,070−14,830	13,700−15,210	*Betula* fruits
BE-5402.1.1	1010.0−1008.0	12,720 ± 170	14,310−15,680	13,650−16,360	*Betula nana* leaf
BE-5403.1.1	1110.0−1105.0	14,000 ± 210	16,340−17,560	15,740−18,160	*Betula nana* fruit, *Betula nana* fruit scale, *Betula nana* leaf
BE-5404.1.1	1340.0−1335.0	15,900 ± 130	18,890−19,520	18,560−19,850	*Salix herbacea* leaf, rhizome indet

[a] Stuiver and Pollach, 1977

[b] Stuiver and Reimer, 1993; Reimer et al., 2013

[c] Bronk Ramsey, 1994, 1995, 2001; Bronk Ramsey et al., 2001; Heegaard et al., 2005

[d] van Raden et al., 2013

1025 **Table 2: Oldest radiocarbon dates from terrestrial plant remains found in sediment sequences from lakes north and south of the Alps. Uncertainties of ^{14}C ages refer to 68% probabilities (1σ) whereas ranges of calibrated ages represent 95% probabilities (2σ).**

Code (Fig. 1a)	Site name	Reference	^{14}C age (BP)[a]	Age (cal BP)[b]	Age range (cal BP)[b]	Material
M	Moossee	This issue	15,900 ± 130	19,180	18,890−19,520	*Salix herbacea* leaf, rhizome indet
1	Burgäschisee	Rey et al., 2017	15,380 ± 70	18,660	18,490−18,800	Twiglet indet
2	Wauwilermoos	Beckmann, 2004	15,300 ± 130	18,560	18,260−18,830	Ericaceae twig
3	Soppensee	Hajdas et al., 1993; Lotter, 1999	14,190 ± 120	17,270	16,900−17,620	Terrestrial plant remains indet
4	Rotsee	Lotter and Zbinden, 1989	14,600 ± 200	17,770	17,250−18,270	Terrestrial plant remains indet
5	Zürichsee	Lister, 1988	14,600 ± 250	17,760	17,110−18,370	Twiglet indet
6	Lago Piccolo di Avigliana	Larocque and Finsinger, 2008	14,930 ± 80	18,150	17,930−18,360	Wood indet
7	Lago di Monate	This issue	16,000 ± 250	19,310	18,780−19,930	Deciduous leaf fragments indet
8	Lago di Origlio	Tinner et al., 1999; Samartin et al., 2012	14,520 ± 80	17,700	17,480−17,930	Wood indet
9	Gola di Lago	This issue	14,640 ± 70	17,820	17,610−18,010	Deciduous leaf, twig fragments
10	Lago d'Iseo	Lauterbach et al., 2012	14,950 ± 130	18,180	17,870−18,500	Terrestrial plant remains indet
11	Lago di Garda	Ravazzi et al., 2014	14,350 ± 70	17,490	17,220−17,710	*Hippophaë* seed, leaf fragment indet
12	Lago di Ragogna	Monegato et al., 2007	14,490 ± 130	17,660	17,310−17,980	*Larix* and *Pinus* remains

[a] Stuiver and Pollach, 1977

[b] Stuiver and Reimer, 1993; Reimer et al., 2013

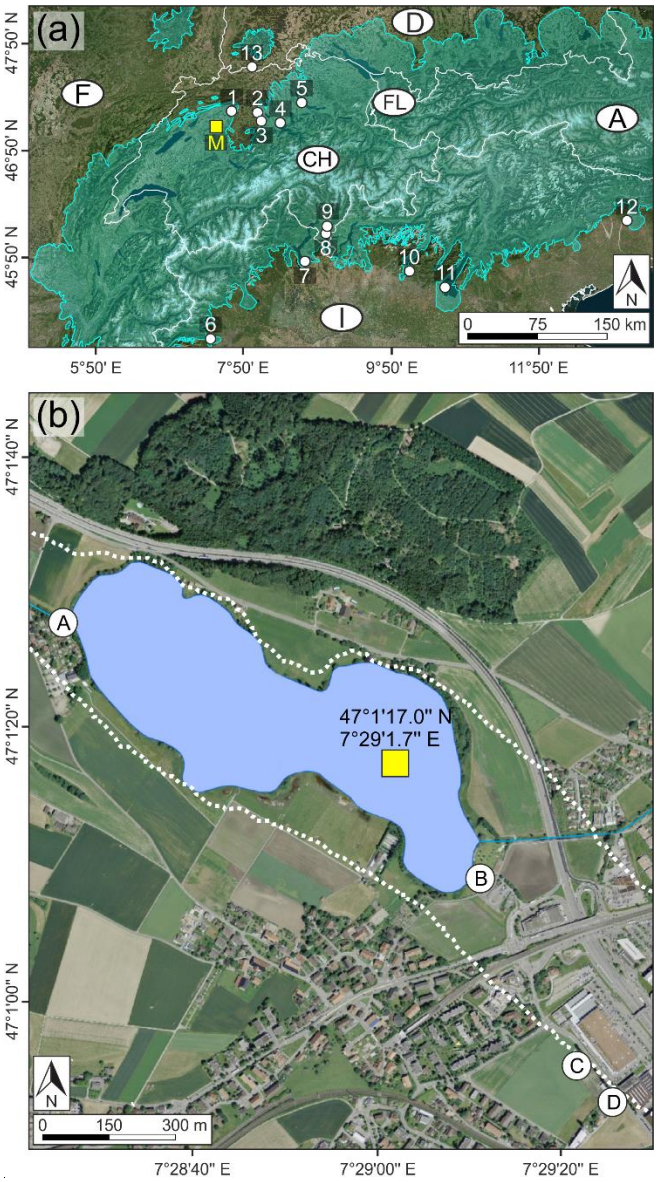

Figure 1: (a) Overview map of Switzerland (CH) and the neighbouring countries (white lines = national borders, source of the satellite image: Google Earth (modified)) including the glacier extent during the Last Glacial Maximum (LGM, light blue area; Ehlers and Gibbard, 2004), the study site Moossee (M, yellow box) and other discussed sites (white circles). 1 Burgäschisee (Rey et al., 2017); 2 Wauwilermoos (Beckmann, 2004); 3 Soppensee (Lotter, 1999); 4 Rotsee (Lotter and Zbinden, 1989); 5 Lake Zurich (Lister, 1988); 6 Lago Piccolo di Avigliana (Larocque and Finsinger, 2008); 7 Lago di Monate (this issue); 8 Lago di Origlio (Tinner et al., 1999); 9 Gola di Lago (this issue); 10 Lago d'Iseo (Lauterbach et al., 2012); 11 Lago di Garda (Ravazzi et al., 2014); 12 Lago di Ragogna (Monegato et al., 2007); 13 Bergsee (Duprat-Oualid et al., 2017). A = Austria, D = Germany, F = France, FL = Liechtenstein, I = Italy. (b) Detailed map of Moossee (blue area = present lake surface area, source of the aerial photograph: swisstopo (modified)), the extent of the former lake area (dotted white line; Harb, 2017), the coring coordinates (yellow box) and local archaeological sites (white circles; Harb, 2017). A Moossee West; B Moossee East; C Moosbühl II; D Moosbühl I.

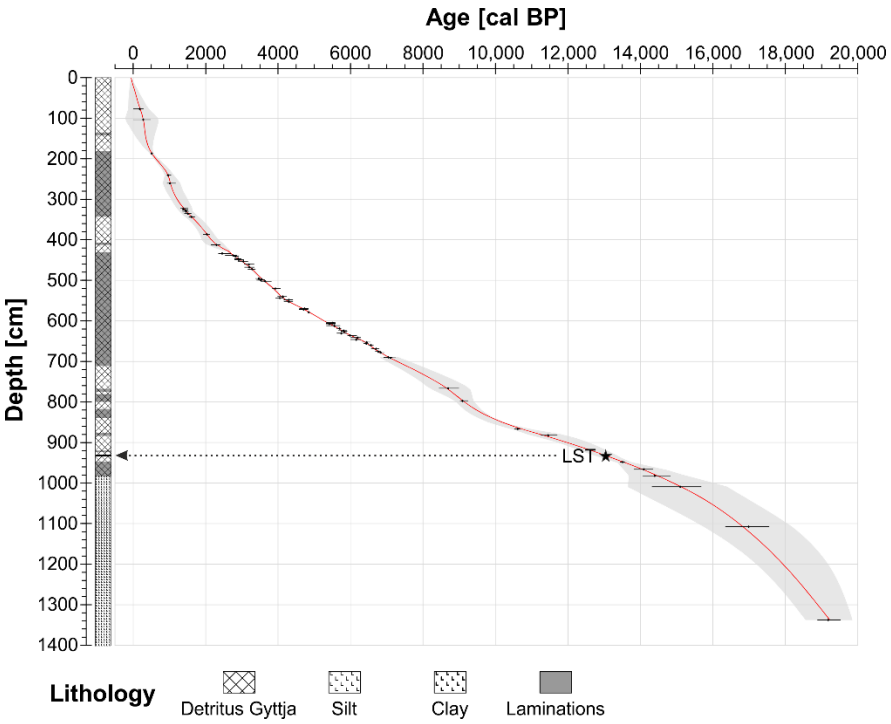

Figure 2. Age-depth model and lithology of Moossee. Black dots show the calibrated ages with 95 % (2σ) probabilities (IntCal13, Reimer et al., 2013). The red line is the modelled chronology using OxCal 4.3 from 435−691 cm (V-sequence, ~~see~~ Bronk Ramsey 1994, 1995, 2001; Bronk Ramsey et al., 2001) and clam 2.2 smooth spline at smoothing level = 0.3 from 0−435 cm and from 691−1335 cm (Blaauw, 2010). The 95 % (2σ) probabilities of the model (grey area) were calculated using again OxCal V-sequence (435−691 cm) and a generalized mixed-effect regression (GAM, 0−435 cm and 691−1335 cm, ~~see~~ Heegaard et al., 2005). LST = Laacher See Tephra (black line at 932−933 cm and black star).

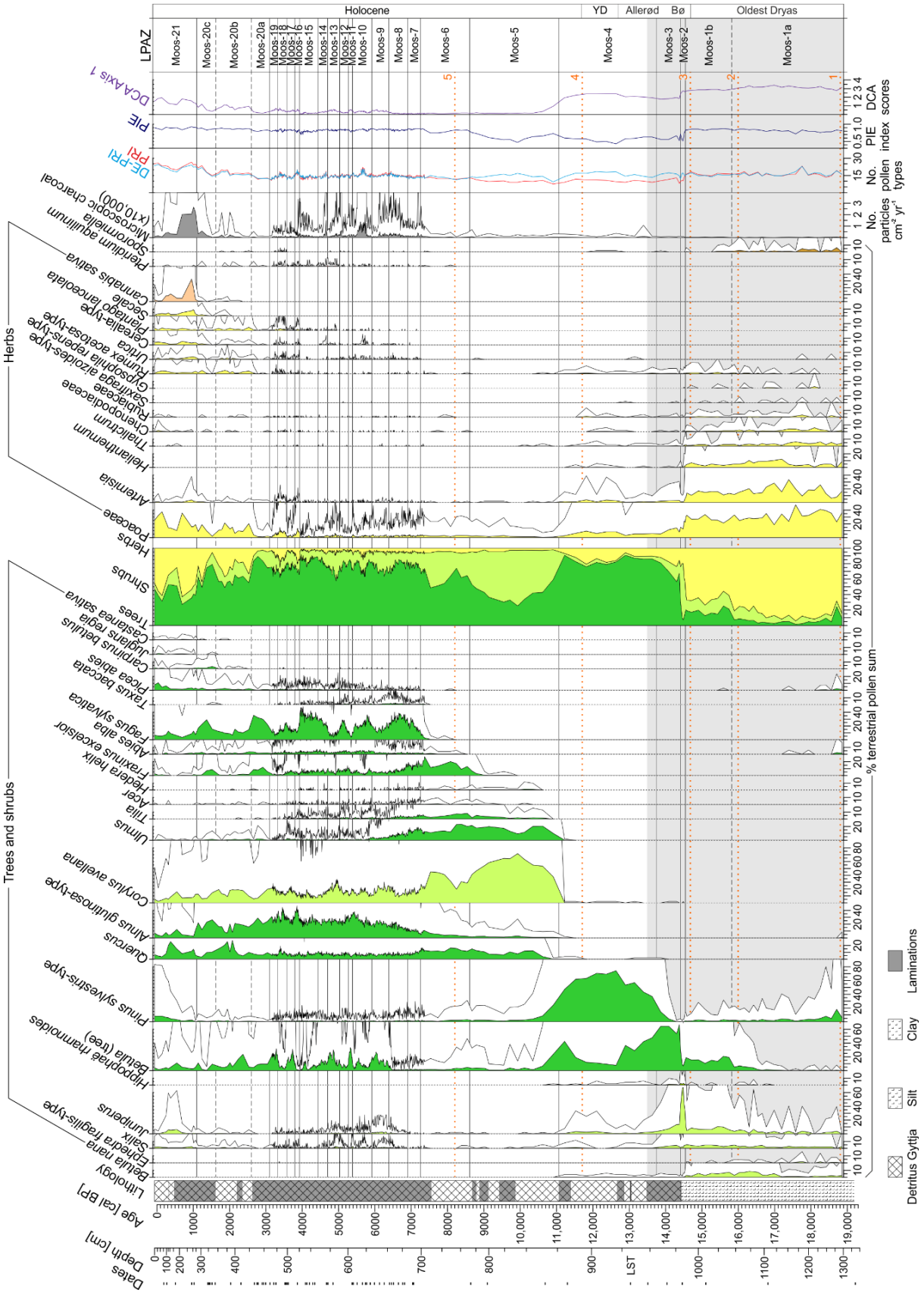

Figure 3. Moossee sediment sequence. Presented are the dates (small black lines), the lithology, percentages of selected pollen types, *Pteridium aquilinum* (fern spore) and *Sporormiella* (coprophilous fungal spore), microscopic charcoal influx values, the palynological richness (PRI, red line), the evenness-detrended palynological richness (DE-PRI, light blue line), the palynological evenness (PIE, dark blue line) as well as the detrended correspondence analysis (DCA, purple line). Empty curves show 10x exaggerations. LST = Laacher See Tephra; Bø = Bølling; YD = Younger Dryas. The horizontal light grey bar indicates the time window of Fig. 4. The orange horizontal dotted lines (1−5) mark important climatic breaks on the basis of temperature changes (see Finsinger et al., 2019) and/ or changing moisture availability (e.g. Joannin et al., 2013). 1 = onset of the Oldest Dryas (19,000 cal BP, Wirsig et al., 2016); 2 = post-HE-1 warming (16,000 cal BP, Samartin et al., 2012); 3 = onset of the Bølling (14,700 cal BP, van Raden et al., 2013); 4 = onset of the Holocene (11,700 cal BP, Heiri et al., 2015); 5 = 8.2 ka event (8200 cal BP, Tinner and Lotter, 2001).

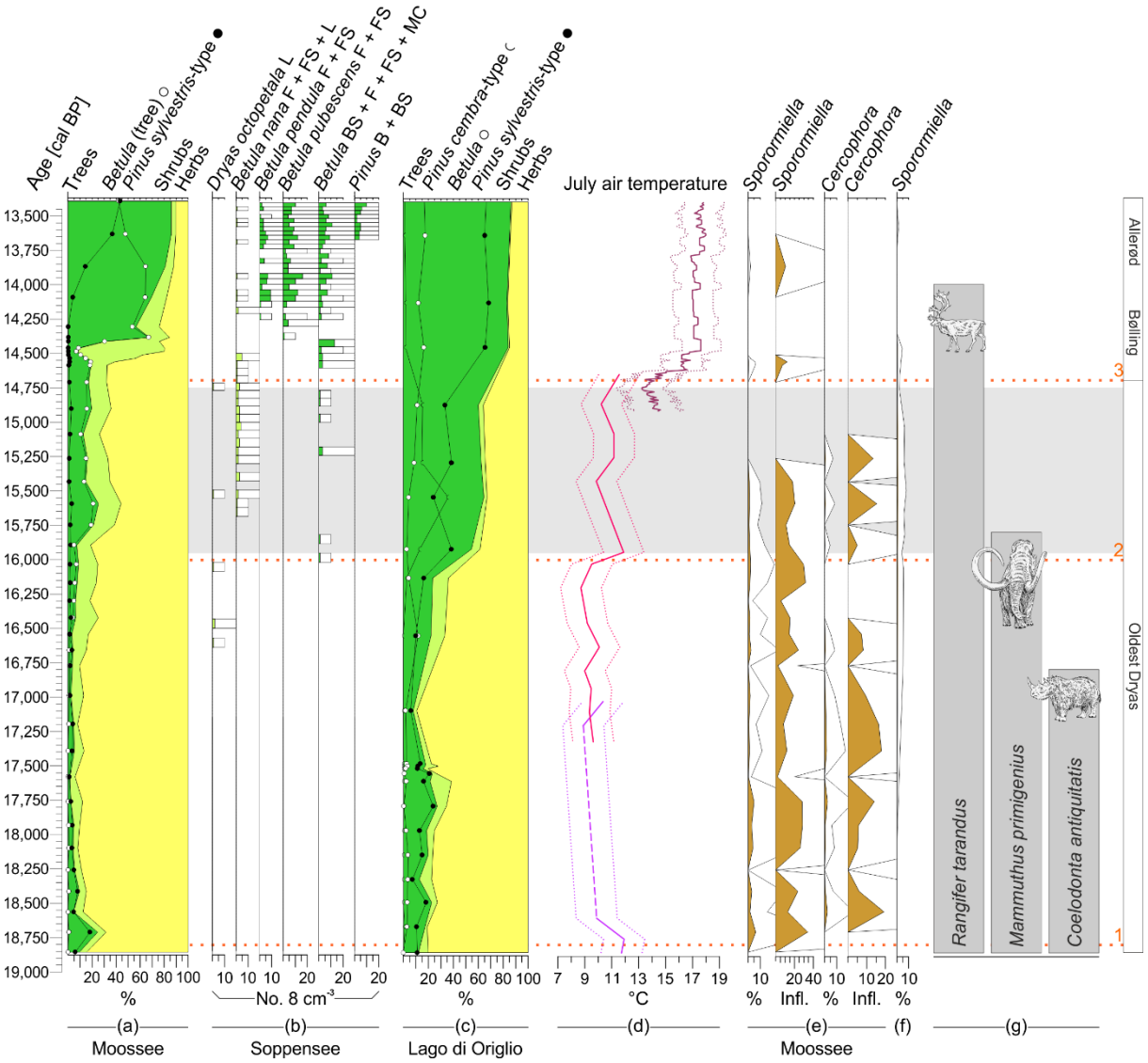

Figure 4. Composite. (a) Main pollen percentages of Moossee including pollen percentages of *Betula* (tree) and *Pinus sylvestris*-type. (b) Concentrations of selected plant macrofossils at Soppensee (Lotter, 1999). B = bud, BS = bud scale, F = fruit, FS = fruit scale, L = leaf, MC = male catkin. (c) Main pollen percentages of Lago di Origlio including pollen percentages of *Betula*, *Pinus sylvestris*-type and *Pinus cembra*-type (Tinner et al., 1999). (d) Mean July air temperature estimates for the altitude of Moossee (521 m a.s.l.) using chironomid-based temperature reconstructions from Lago della Costa (light purple lines, Samartin et al., 2016), Lago di Origlio (pink lines, Samartin et al., 2012) and a chironomid-inferred stacked temperature record representing mean July air temperature estimates in the Northern and Central Swiss Alps (dark red lines, Heiri et al., 2015). Temperatures were corrected under the assumption of a constant modern temperature rate of 6 °C km^{-1} (Livingstone and Lotter, 1998) and plotted according to Finsinger et al. (2019). The Origlio record is only shown for the oldest part (older than 14,600 cal yr BP). Dotted lines reflect standard error estimates. (e) *Sporormiella* and *Cercophora* percentages and influx values (spores cm^{-2} yr^{-1}) of Moossee. (f) *Sporormiella* percentages of Burgäschisee (Rey et al., 2017). (g) Presence and extinction of important Pleistocene megafauna (Nielsen, 2013; Cupillard et al., 2015). The horizontal light grey bar indicates the time window of local archaeological findings (reindeer hunter camps, Bullinger et al., 1997; Harb, 2017; Nielsen, 2018). Empty curves show 10x exaggerations (b, e, f). The orange horizontal dotted lines (1−3) mark important climatic breaks on the basis of temperature changes (~~see~~ Finsinger et al., 2019). 1 = onset of the Oldest Dryas (19,000 cal BP, Wirsig et al., 2016); 2 = post-HE-1 warming (16,000 cal BP, Samartin et al., 2012); 3 = onset of the Bølling (14,700 cal BP, van Raden et al., 2013).

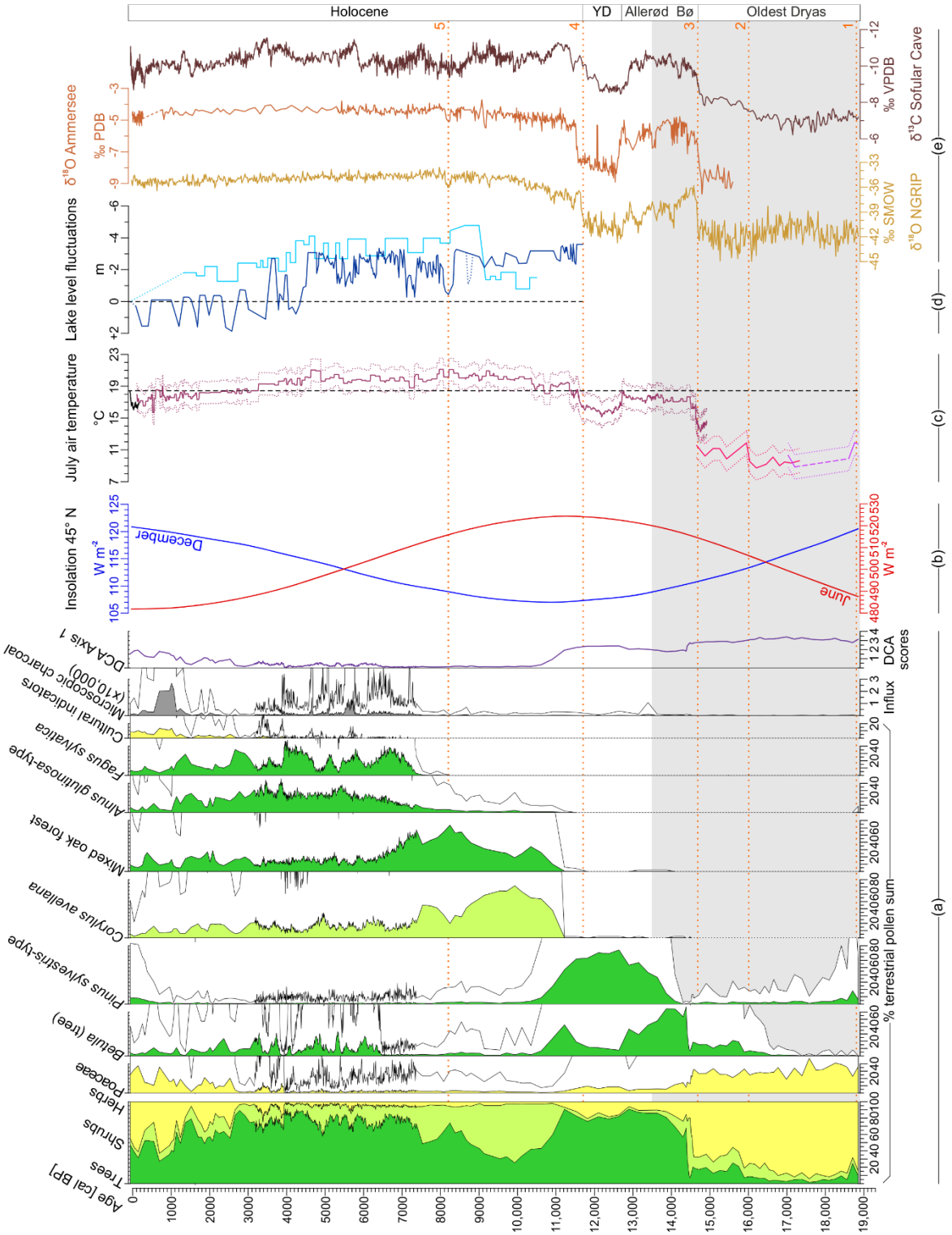

Figure 5. Composite. (a) Selected pollen percentages, microscopic charcoal influx values (particles cm^{-2} yr^{-1}) and the detrended correspondence analysis (DCA, purple line) of Moossee. Mixed oak forest = Σ *Quercus* + *Ulmus* + *Fraxinus excelsior* + *Tilia* + *Acer*. Cultural indicators = Σ Cerealia-type + *Plantago lanceolata*. Empty curves show 10x exaggerations. (b) June (red line) and December (blue line) insolation for 45°N (Berger and Loutre, 1991). (c) Mean July air temperature estimates for the altitude of Moossee (521 m a.s.l.) using chironomid-based temperature reconstructions from Lago della Costa (light purple lines, Samartin et al., 2016), Lago di Origlio (pink lines, Samartin et al., 2012) and a chironomid-inferred stacked temperature record representing mean July air temperature estimates in the Northern and Central Swiss Alps (dark red lines, Heiri et al., 2015). Additionally, historical (1755–2018 AD) 30-yr moving average July air temperature measurements from Basel-Binningen (black line) are shown. Temperatures were corrected under the assumption of a constant modern temperature rate of 6 °C km^{-1} (Livingstone and Lotter, 1998) and plotted according to Finsinger et al. (2019). The black vertical dashed line indicates today's average July air temperatures (= 18.3 °C) in Bern/ Zollikofen (MeteoSwiss, 2017). The Origlio record is only shown for the oldest part (older than 14,600 cal yr BP). Dotted lines reflect standard error estimates. (d) Relative lake level reconstructions of Lac de Cerin (light blue line, Magny et al., 2011) and Lago di Ledro (dark blue line, Magny et al. 2012). The black vertical dashed line mark today's lake levels. (e) Stable isotopes records from NGRIP (light brown line, North Greenland Ice Core Project members, 2004), Ammersee (dark orange line, von Grafenstein et al., 1998, 1999) and Sofular Cave (brown line, Fleitmann et al., 2009). The horizontal light grey bar indicates the time window of Fig. 4. The orange horizontal dotted lines (1–5) mark important climatic breaks on the basis of temperature changes (~~see~~ Finsinger et al., 2019) and/ or increased moisture availability (e.g. Joannin et al., 2013). 1 = onset of the Oldest Dryas (19,000 cal BP, Wirsig et al., 2016); 2 = post-HE-1 warming (16,000 cal BP, Samartin et al., 2012); 3 = onset of the Bølling (14,700 cal BP, van Raden et al., 2013); 4 = onset of the Holocene (11,700 cal BP, Heiri et al., 2015); 5 = 8.2 ka event (8200 cal BP, Tinner and Lotter, 2001). Bø = Bølling; YD = Younger Dryas.